Supplementary Information

for

Towards ^{213}Bi alpha-therapeutics and beyond: Unraveling the foundations of efficient Bi(III) complexation by DOTP

Dávid Horváth,[a] Fabio Travagin,[b] Nicol Guidolin,[c] Federica Buonsanti,[c] Gyula Tircsó,[a] Imre Tóth,[a,d] Frank Bruchertseifer,[e] Alfred Morgenstern,[e] Johannes Notni,[f,g] Giovanni B. Giovenzana,[b,h,*] Zsolt Baranyai [c,*]

[a] Department of Physical Chemistry, University of Debrecen, H - 4010, Debrecen, Egyetem tér 1., Hungary
[b] Dipartimento di Scienze del Farmaco, Università del Piemonte Orientale "A. Avogadro"
Largo Donegani 2/3, Novara, Italy
[c] Bracco Research Center, Bracco Imaging SpA, Via Ribes 5, 10010 Colleretto Giacosa (TO), Italy
[d] Department of Inorganic and Analytical Chemistry, University of Debrecen, H-4010, Debrecen, Egyetem tér 1., Hungary
[e] European Commission, Joint Research Centre (JRC), Karlsruhe, Germany
[f] Institute of Pathology, Klinikum rechts der Isar, Technische Universität München, Trogerstr. 18, 81675 München, Germany
[g] Experimental Radiopharmacy, Clinic for Nuclear Medicine, University Hospital Essen, Hufelandstr. 55, 45147 Essen, Germany.
[h] CAGE Chemicals, Via Bovio 6, 28100 Novara, Italy

*Corresponding Authors:

Giovanni B. Giovenzana
Dipartimento di Scienze del Farmaco, Università del Piemonte Orientale "A. Avogadro"
Largo Donegani 2/3,
Novara, Italy
Tel. +390321375 846/746
E-mail: giovanni.giovenzana@uniupo.it

Zsolt Baranyai
Bracco Imaging SpA, Bracco Research Center,
Via Ribes 5,
10010, Colleretto Giacosa (TO), Italy.
Tel. +390403757842
E-mail: zsolt.baranyai@bracco.com

Keywords: bismuth / chelating agent / Thermodynamic / Kinetics / α emission /theranostics

Manuscript Classifications: Chelates; Bismuth; Coordination Chemistry; Radiochemistry

I. Protonation and complexation equilibria of $DOTA^{4-}$, $DOTP^{8-}$ and NTA^{3-} ligands

I.1. Experimental

The chemicals used for the experiments were of analytical grade. $Bi(ClO_4)_3$ solution was prepared by dissolving Bi_2O_3 (99.9%, Fluka) in 6 M $HClO_4$. The concentration of the $Bi(ClO_4)_3$ solution was determined by complexometry with a standardized Na_2H_2EDTA solution and xylenol orange as indicator at about pH 1. The H^+ concentration of the $Bi(ClO_4)_3$ solution was determined by using pH potentiometric titration in the presence of a twofold excess of Na_2H_2EDTA. H_4DOTA and H_3NTA were purchased from *Sigma*, while H_8DOTP and H_4AAZTA ligands were synthesized according to literature procedures[1,2]. HP-DO3A was provided by *Bracco Imaging S.p.A.*. The concentration of the ligand stock solutions was determined by pH-potentiometric titration in the presence and absence of a large (40-fold) excess of $CaCl_2$. The pH-potentiometric titrations were made with standardized 0.2 M NaOH. The solutions of the Bi^{III} complexes were prepared by the reaction of equivalent amounts of $Bi(ClO_4)_3$ and the ligand. The $Bi(ClO_4)_3$ solution was slowly added dropwise to the vigorously stirred solution of Na_2H_2DOTA, Na_6H_2DOTP or Na_2HHP-DO3A. The pH of the solution was controlled, and it was set to 5-5.5 by addition of concentrated NaOH solution. *Caution! Dry powder perchlorate samples are prone to explosion and should be handled with special care, especially in larger quantities.*

The protonation constants of the ligands and the Bi^{III} complexes were determined by pH potentiometric titration with 0.2 M NaOH at 25°C using a constant ionic strength (0.15 M $NaClO_4$) in 6 mL samples. The concentration of the ligand and Bi^{III} complexes was generally 0.002 M. For the pH measurements and titrations, *Metrohm 888 Titrando* titration workstation equipped with *Metrohm-6.0234.110* combined electrode was used. The solutions were stirred, and N_2 was bubbled through them. The titrations were made in the pH range of 1.7-12.0. KH-phthalate (pH=4.005) and borax (pH=9.177) buffers were used to calibrate the pH meter. For the calculation of $[H^+]$ from the measured pH values, the method proposed by *Irving et al.* was used as follows:[3] 0.01 M $HClO_4$ solution was titrated with standardized NaOH solution at 0.15 M $NaClO_4$ ionic strength. The differences (A) between the measured (pH_{read}) and calculated pH ($-\log[H^+]$) value (*i.e.*, the average of A values in the pH-range of 1.75-2.20 was used to obtain the equilibrium H^+ concentration from the pH values measured in the titration experiments (A=-0.042). For the equilibrium calculations, the stoichiometric water ionic product (pK_w) was also needed to calculate $[OH^-]$ values under basic conditions. The V_{NaOH} – pH_{read} data pairs of the $HClO_4$ – NaOH titration obtained in the pH range 10.8 – 12.0 were used to calculate the pK_w value (pK_w=13.65).

The stability constants of the $[Bi(DOTA)]^-$, $[Bi(DOTP)]^{5-}$, $[Bi(NTA)]$ and $[Bi(NTA)_2]^{3-}$ complexes were determined by spectrophotometry at the absorption band of Bi^{III} complexes in the wavelength range of 210-350 nm. For Bi^{III} - NTA systems, two series of samples were prepared with $[Bi^{III}]_{tot}$=0.1 mM and $[NTA]_{tot}$=0.1 mM or $[Bi^{III}]_{tot}$=0.1 mM and $[NTA]_{tot}$=0.2 mM in 0.15 M $NaClO_4$ solution. In the first series the -log$[H^+]$ values were adjusted to 0.1, 0.3, 0.6 and 1.0 M with the addition of calculated amounts of 3.0 M $HClO_4$ (ionic strength was not constant in these samples). In the second series, the pH values of the samples were adjusted by stepwise addition of the concentrated NaOH and $HClO_4$ solutions in the pH range 2.0 – 5.5. For Bi^{III} - DOTA - NTA systems, six samples were prepared with $[Bi^{III}]_{tot}$=50 μM, $[NTA]_{tot}$=50 mM and $[DOTA]_{tot}$=0.0, 20, 40, 60, 80 and 100 μM in 0.15 M $NaClO_4$ solution. For Bi^{III} - DOTP - NTA systems, eight samples were prepared with $[Bi^{III}]_{tot}$=50 μM, $[NTA]_{tot}$=10 mM and $[DOTP]_{tot}$=0.0, 30, 60, 90, 120, 150, 210 and 300 μM in 0.15 M $NaClO_4$ solution. The pH values of the samples were adjusted to 3.0 by stepwise addition of the concentrated NaOH and/or $HClO_4$ solutions. The samples were kept for a week at 50 °C and eight weeks at 25 °C in order to attain equilibrium. The time needed to reach the equilibria was determined by spectrophotometry and the absorbance values of the samples were determined than determined for the samples containing $[Bi(NTA)]$, $[Bi(NTA)_2]^{3-}$, $[Bi(DOTA)]^-$ and $[Bi(H_4DOTP)]^-$ complexes ($[Bi(H_4DOTP)]^-$ species predominates at pH=3.0). For the calculations of the stability constants of the Bi^{III} complexes, the molar absorptivities of $[Bi(NTA)]$, $[Bi(NTA)_2]^{3-}$, $[Bi(DOTA)]^-$ and $[Bi(H_4DOTP)]^-$ species were determined by recording the spectra of 0.01, 0.05, 0.1 and 0.2 mM solutions of $[Bi(NTA)]$, $[Bi(NTA)_2]^{3-}$, $[Bi(DOTA)]^-$ and $[Bi(H_4DOTP)]^-$at 295, 297, 300, 303, 305, 308, 310, 312, 315, 317 and 320 nm in the presence of 0.15 M $NaClO_4$ ($[Bi(NTA)]$ was prepared at pH=2.0 in the presence of two fold NTA excess). The spectrophotometric measurements were made by *PerkinElmer Lambda 365* UV-Vis spectrophotometer at 25 °C, using 1.0 cm cells. The protonation and stability constants were calculated with the PSEQUAD program.[4]

Explicit hydrogen atoms and overall charges of the chelating agents and complexes thereof are used only when relevant to the discussion, otherwise omitted for brevity.

I.2 Acid-base properties of $DOTA^{4-}$, $DOTP^{8-}$ and NTA^{3-} ligands.

The protonation constants of ligands, defined by Eq. (S1), have been determined by pH-potentiometry, ^1H- and ^{31}P-NMR spectroscopy.

$$K_i^H = \frac{[H_iL]}{[H_{i-1}L][H^+]} \tag{S1}$$

where i=1, 2…7. The protonation constant of DOTP has also been determined by ^{1}H-and ^{31}P NMR spectroscopy, recording the chemical shift variations of the non-labile protons and phosphorous atoms as a function of pH. The ^{1}H- and ^{31}P-NMR titration curves (Figure S1) display sharp changes at certain pH values, which are related to the protonation/deprotonation of the ligand. Since the protonation/deprotonation is fast on the NMR time scale, the chemical shifts of the observed signals represent a weighted average of the shifts of the different species involved in a specific protonation step (Eq. (S2)):[5]

$$\delta_{obs} = \sum x_i \delta^{H_iL} \tag{S2}$$

where, δ_{obs} is the observed chemical shift of a given signal (^{1}H and ^{31}P), x_i and δ^{H_iL} are the molar fraction and the chemical shift of the involved species, respectively. The observed chemical shifts (δ_{obs}) have been fitted to the Eq. (S2), respectively (the molar fractions x_i and the concentration of the different protonated species have been expressed by the protonation constants K_i^H, Eq. (S1)). The fittings of the experimental data points are shown in Figures S1 and S2. The obtained logK_i^H values are listed in Table S1.

Table S1. Protonation constants of **NTA^{3-}**, **$DOTA^{4-}$** and **$DOTP^{8-}$** at 25°C

	NTA^{3-}		**$DOTA^{4-}$**			**$DOTP^{8-}$**	
	0.15 M $NaClO_4$	**1.0 M $NaClO_4$[a]**	**0.15 M $NaClO_4$**	**0.15 M NaCl [b]**	**0.1 M $Me_4N(NO_3)$ [c]**	**0.15 M $NaClO_4$**	**0.1 M $Me_4N(NO_3)$[d]**
logK_1^H	9.22 (2)	8.96	9.12 (1)	9.14	12.09	*13.6 (1)	14.65
logK_2^H	2.80 (2)	2.20	9.50 (1)	9.21	9.76	*12.21 (4)	12.40
logK_3^H	1.06 (3)	1.98	4.51 (1)	4.48	4.56	8.62 (2)	9.28
logK_4^H	–	1.10	4.05 (1)	4.03	4.09	7.53 (2)	8.09
logK_5^H	–	–	2.05 (1)	1.99	–	5.82 (3)	6.12
logK_6^H	–	–	1.14 (2)	–	–	5.11 (3)	5.22
logK_7^H	–	–	–	–	–	1.64 (3)	–

[a] Ref. [6]; [b] Ref. [7]; [c] Ref. [8]; [d] Ref. [9]; * ^{1}H and ^{31}P NMR spectroscopy.

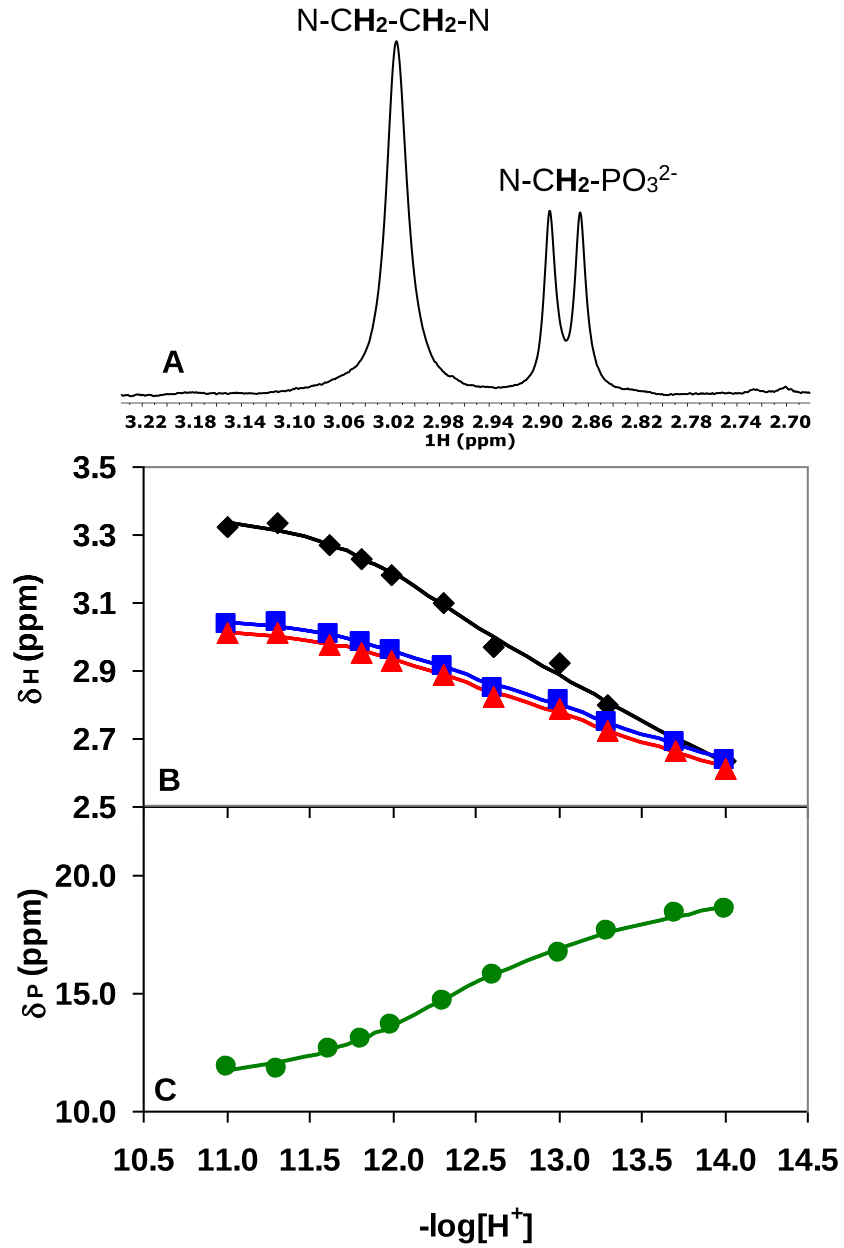

Figure S1. 400 MHz ^{1}H-NMR spectra (**A**) at pH = 11.0 and the chemical shifts of the ring (◆) and the phosphonate (■, ▲) –CH$_2$- protons (**B**) and 162 MHz ^{31}P NMR shift of phosphorous atoms (●) of DOTP^{8-} ligand at different pH (**C**). The solid lines and the symbols represent the calculated and the experimental δ_H and δ_P values, respectively ([DOTP]$_{tot}$=10 mM, pH=12.6, H_2O, 0.15 M $NaClO_4$ at pH<12, ionic strength of the samples was not constant at pH>12, 25°C)

The protonation of DOTA-like ligands is fully characterized with both spectroscopic and potentiometric methods.[9–12] These studies reveal that the first and second protonation processes occur at two opposite ring nitrogen atoms, whereas the third and fourth protonation steps take place at the carboxylate/basic phosphonate groups of the pendant arms attached to the non-protonated ring nitrogen atoms, because of the greater charge separation and lower electrostatic repulsion between the protonated donor atoms.[9,10] Further protonation processes occur on the non-protonated carboxylate/basic phosphonate groups of H_4DOTA and H_4DOTP^{4-} ligands.[9,10] Less basic phosphonate groups of H_6DOTP^{2-} might be protonated at pH<2. Since the deprotonation of the ring nitrogen atoms in H_2DOTP^{6-} species takes place at pH>12, the accurate determination of the protonation constants can not be performed by pH-potentiometry. $\log K_1^H$ and $\log K_2^H$ values of $DOTP^{8-}$ ligand were determined by ^1H- and ^{31}P-NMR spectroscopy (Figure S1). In the ^1H-NMR spectra of $DOTP^{8-}$ there are only two signals, which can be assigned to the ring methylene protons of the macrocycle (a singlet) and the methylene protons of the phosphonate group (a doublet, $^2J_{PH}$=9.8 Hz), respectively. Starting from the basic side, the addition of the first and the second equivalent of acid to $DOTP^{8-}$ results in a significant downfield shift of the ^1H NMR signals of both the ring and phosphonate methylene protons and the upfield shift of the ^{31}P NMR signal of the phosphonate group. Since the largest changes of the chemical shifts take place on the ^1H NMR signals of the ring methylene protons, it can be safely assumed that the first and second protonation processes occur at two opposite ring nitrogen atoms of the $DOTP^{8-}$ ligand.

Comparison of the related protonation constants of DOTA indicates that the $\log K_i^H$ values obtained in 0.15 M $NaClO_4$ and 0.15 M NaCl solutions are essentially identical confirming the negligible influence of the anions of the background electrolyte for the protonation constants of the ligand. On the other hand, the $\log K_1^H$ value of DOTA and DOTP obtained in 0.15 M $NaClO_4$ or 0.15 M NaCl is lower by about 3 and 1 log unit/s than the constant determined in 0.1 M $Me_4N(NO_3)$ solutions. The lower $\log K_1^H$ value of DOTA and DOTP obtained in $NaClO_4$ or NaCl solutions can be interpreted by the formation of the relatively stable Na^I-complexes (e.g. $\log K_{Na(DOTA)}$=4.38).[13]

Interestingly, the single resonance in ^{31}P-NMR spectrum of H_6DOTP^{2-} is broadened and split into two resonances of equal area separated by about 14 ppm by lowering the temperature from 313 K to 253 K at pH=2.5 in DMSO-D_6/H_2O: 40/60 vol % mixture (Figure S2). A similar behaviour for H_xDOTP^{x-8} has been identified at pH=7.0 (x=3 - 6).[1] By taking into account the structure of H_6DOTP^{2-} species, it can be assumed that the broadening and coalescence of ^{31}P NMR signals is caused by the increased exchange rate of non-H-bonded and H-bonded phosphonate pendants with the protonated ring nitrogen atoms (Scheme S1). The ^{31}P-NMR signals of the $-\mathbf{P}O_3H^-$ group were suitable for carrying out line-shape analysis by simulating the ^{31}P-NMR spectra obtained at different temperatures. The transverse relaxation time (T_2) of the $-\mathbf{P}O_3H^-$ phosphorus signal was found to be T_2=0.016 s. The experimental spectra have been simulated using the chemical shift difference of the two phosphorous signals (Δδ=2271 Hz). Examples for typical experimental and simulated spectra are shown in Figure S2.

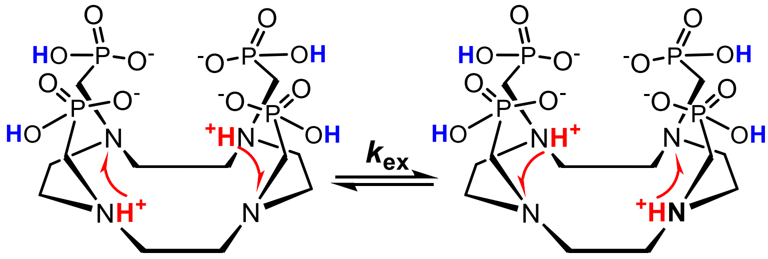

Scheme S1. Fluxional rearrangement of the H_6DOTP^{2-} species.

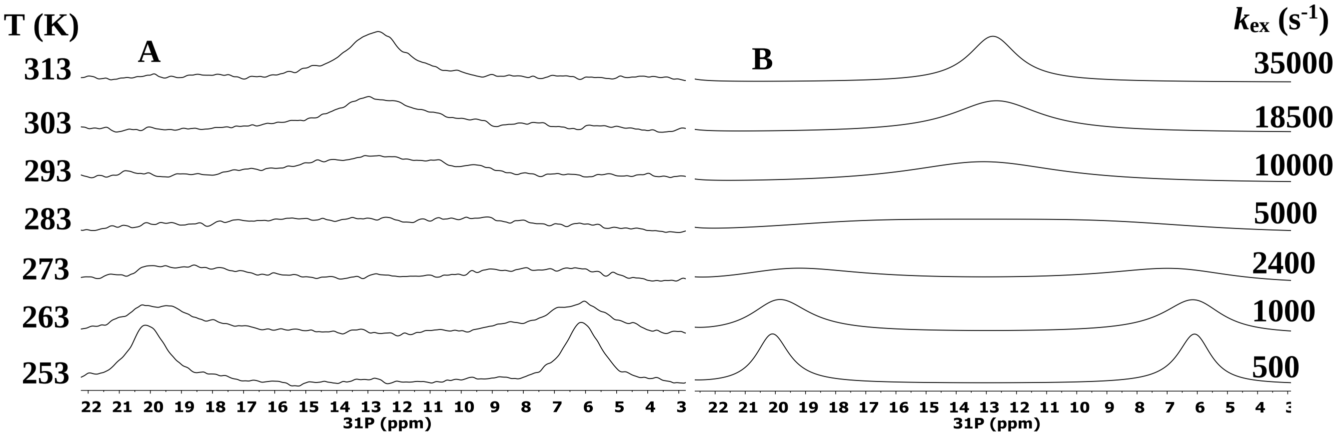

Figure S2. Experimental (**A**) and simulated (**B**) 162 MHz ^{31}P NMR spectra of H_6DOTP^{2-} in DMSO-D_6/ H_2O: 40/60 vol % mixture ($[H_6DOTP]_{tot}$=5.0 mM, 162 MHz, pH=2.5)

The activation parameters (Table S2) of the fluxional rearrangement for H_6DOTP^{2-} species have been estimated with the *Eyring* equation by using the k_{ex} rate constant obtained by the line-shape analysis The *Eyring* plot for the determination of the activation parameters for H_6DOTP^{2-} species is shown in Figure S3.

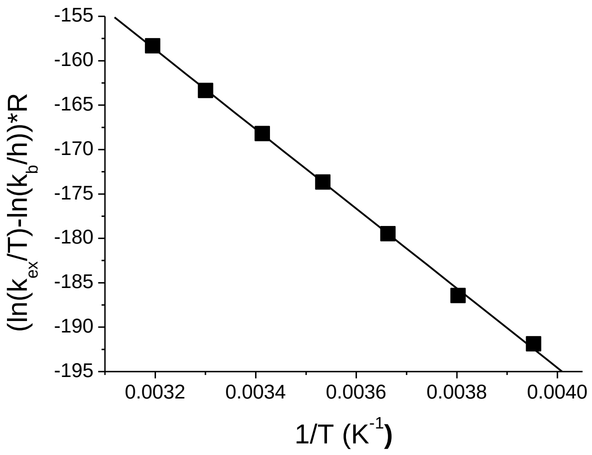

Figure S3. *Eyring* plots for determining the activation parameters of the fluxional rearrangement of H_6DOTP^{2-} species.

Table S2. Rate constants and activation parameters of the isomerization process for H_6DOTP^{2-} species obtained from the line-shape analysis of the ^{31}P-NMR spectra.

	H_6**DOTP**$^{2-}$
$\Delta H^{\ddagger}$ /kJ·mol^{-1}	45 ± 1
$\Delta S^{\ddagger}$ / J·mol^{-1}K^{-1}	-15 ± 2
$\Delta G^{\ddagger}_{298}$ /kJ·mol^{-1}	49 ± 1
k_{ex}^{298} /s^{-1}	13226

The activation energy ($\Delta G^{\ddagger}_{298}$) of the fluxional rearrangement of the H_6DOTP^{2-} is 45 kJ·mol^{-1}, which is somewhat lower than that of H_xDOTP^{x-8} x=3-5 mixture obtained at pH=7.0 ($\Delta G^{\ddagger}_{298}$=56 kJ·mol^{-1}).[1] The lower $\Delta G^{\ddagger}_{298}$ value of H_6DOTP^{2-} might be explained by the protonation of the phosphonate pendants results in the weaker interaction between the non-protonated phosphonate-O$^-$ and the protonated ring nitrogen donor atoms. Our band shape analysis provides negative activation entropy ($\Delta S^{\ddagger}$), which is probably related to the reorganization of the hydration shell around the negatively charged oxygen donor atoms of the phosphonate pendants in the transition state.

I.3 Equilibrium studies of the Bi^{III} - NTA system.

Stepwise and cumulative stability constants of Bi^{III} complexes of NTA^{3-}, defined by Eqs. (S3) and (S4), were determined by spectrophotometry at 25 ºC in 0.15 M $NaClO_4$ solution.

$$K_{BiL} = \frac{[BiL]}{[Bi^{III}][L]} \qquad (S3)$$

$$\beta_{BiL} = \frac{[BiL_2]}{[Bi^{III}][L]^2} \qquad (S4)$$

The K_{BiL} and β_{BiL2} values have been calculated from the spectrophotometric titration data obtained at 1:1 and 1:2 metal to ligand concentration ratio. The equilibrium reaction (Eq. (S5)) has been studied in the –log[H$^+$] range of 0.0 – 5.3 (the ionic strength were constant I=[$NaClO_4$]+[$HClO_4$]=0.15 in the samples [H$^+$]≤0.15 M), where the formation of Bi^{III}, BiL, BiL_2 and H_xL species was assumed (x=1 – 3, y=1 or 2, z = 0 or -3). Some characteristic absorption spectra of Bi^{III} - NTA systems are shown in Figure S4.

$$Bi^{3+} + yH_xNTA^{x-3} \rightleftharpoons [Bi(NTA)_y]^z + x\times y\ H^+ \qquad (S5)$$

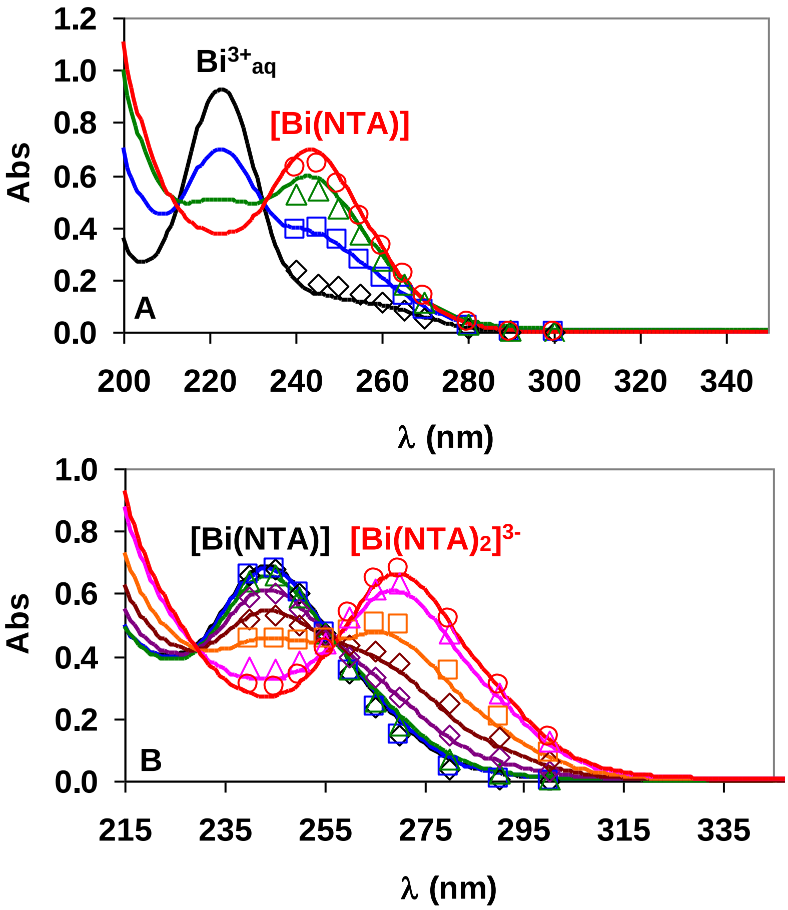

Figure S4. Absorption spectra of the Bi^{III} - NTA system at 1:1 (**A**) and 1:2 (**B**) metal to ligand concentration ratio. The solid lines and the open symbols represent the experimental and the calculated absorbance values, respectively. (**A**: [Bi^{III}]$_{tot}$=[NTA]$_{tot}$=0.1 mM, -log[H$^+$]=**0.1**, **0.3**, **0.6** and **1.0** M (ionic strength was not constant in these samples); **B:** [Bi^{III}]$_{tot}$=0.1 mM, [NTA]$_{tot}$=0.2 mM, pH=**2.01**, **2.41**, **2.95**, **3.52**, **3.96**, **4.42** and **5.15**, 0.15 M NaClO$_4$; l=1 cm, 25°C)

Stability constants of the [Bi(NTA)] and [Bi(NTA)$_2$]$^{3-}$ complexes at 25°C in 0.15 M NaClO$_4$ solution are found to be K_{BiL}=16.97 (3) and β_{BiL2}=26.20 (6), which are in a good agreement with the K_{BiL}=17.53 and β_{BiL2}=26.56 values obtained at 25°C in 1.0 M NaClO$_4$ solution by Karadakov and co-workers.[6]

II. Species distribution of the Bi^{3+} - $DOTA^{4-}$ and Bi^{3+} - $DOTP^{8-}$ systems.

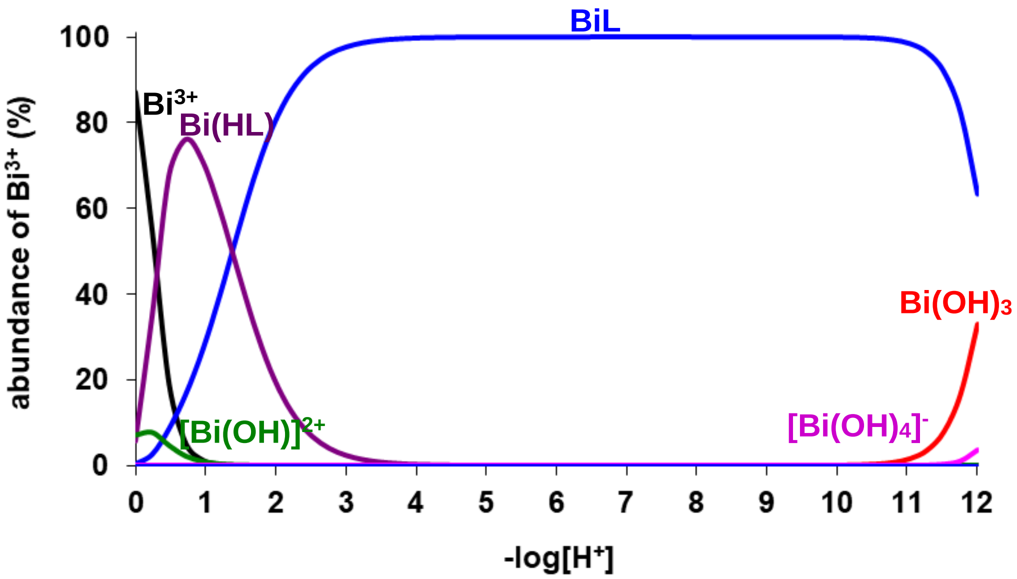

Figure S5. Species distribution of Bi^{3+} - $DOTA^{4-}$ system ([Bi^{3+}]=[$DOTA^{4-}$]=1.0 mM, 0.15 M $NaClO_4$, 25°C)

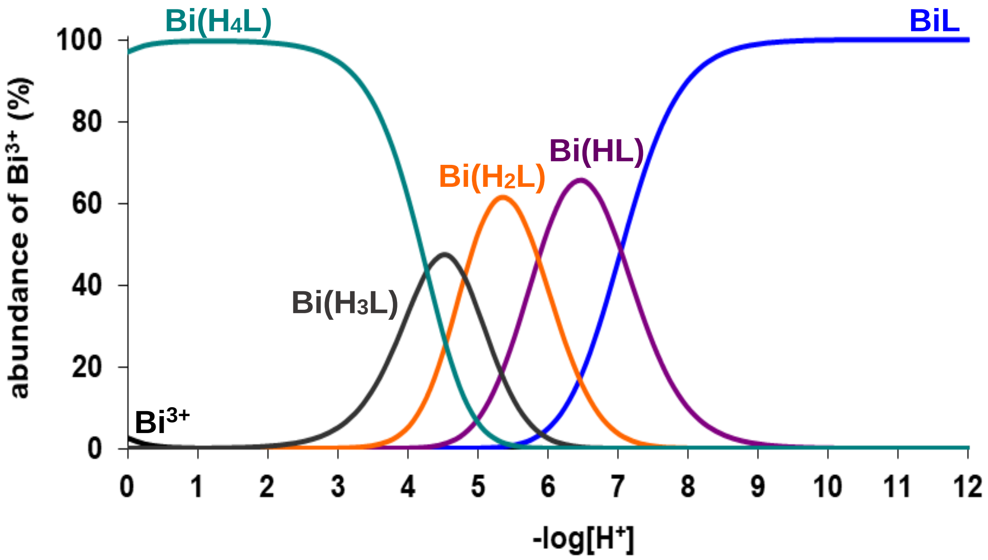

Figure S6. Species distribution of Bi^{3+} - $DOTP^{8-}$ system ([Bi^{3+}]=[$DOTP^{8-}$]=1.0 mM, 0.15 M $NaClO_4$, 25°C)

III. Formation kinetic studies of $[Bi(DOTA)]^-$ and $[Bi(H_xDOTP)]^{x-5}$ complexes (x=0 – 4).

III.1 Experimental

Formation rates of $[Bi(DOTA)]^-$ and $[Bi(H_xDOTP)]^{x-5}$ were studied by spectrophotometry at 308 nm in the presence and absence of citrate as an auxiliary ligand. The formation of $[Bi(DOTA)]^-$ was followed with a *PerkinElmer Lambda 365* UV-Vis spectrophotometer at 25

°C, using 1.0 cm cells (pH=3.3–5.9), whereas the formation of $[Bi(H_xDOTP)]^{x-5}$ was monitored with Applied Photophisics DX-17MV stopped-flow instrument using l=1.0 cm (pH=3.0–5.6) at 25°C in the presence of 0.15 M $NaClO_4$. The formation of Bi^{III} complexes were studied in the presence of a 2 to 40-fold ligand excess in order to assure the pseudo-first-order conditions ($[Bi^{III}]_{tot}$=25 μM). The effect of citrate for the formation rate of $[Bi(DOTA)]^-$ and $[Bi(H_xDOTP)]^{x-5}$ was studied in the presence of 0.05 – 2.0 mM citrate in the pH range 3.0 – 5.6 ($[Bi^{3+}]_{tot}$=25 μM, $[DOTA]_{tot}$=1.0 mM, $[DOTP]_{tot}$=0.1 mM, 0.15 M $NaClO_4$, 25°C). pH values were maintained constant by the application of 0.01 M buffers (Chloroacetic acid (CA), N-methyl-piperazine (NMP), *N,N*-dimethyl-piperazine (DMP), 2-(*N*-morpholino)ethanesulfonate (MES)). The pseudo-first-order rate constants (k_{obs}) were calculated by fitting the absorbance values to the Eq. (S6):

$$A_\mathrm{t} = (A_0 - A_\mathrm{e})\mathrm{e}^{(-k_\mathrm{obs}\mathrm{t})} + A_\mathrm{e} \qquad (S6)$$

where A_0, A_e and A_t were the absorbance values at the start (t=0 s), at equilibrium and at the t time of the reaction, respectively. The calculations were performed by using the computer program Micromath Scientist, version 2.0 (Salt Lake City, UT, USA).

The diprotonated $*[Bi(H_2DOTP)]^{3-}$ intermediate was studied by following the ΔpH with spectrophotometry at 506 nm in the presence of methyl-orange as indicator in the Bi^{III}-H_6DOTP^{2-} reaction system ($[Bi^{III}]_{tot}$=0.5 mM, $[H_6DOTP^{2-}]$, $[\text{methyl orange}]_{tot}$=12.5 μM, pH_{end}=3.17, 0.15 M $NaClO_4$, 0°C). ΔpH was calculated by considering the absorbance values of the Bi^{3+}-H_6DOTP^{2-} reaction system at the start (A_0) and at equilibrium (A_e). A_0 and A_e were calculated by fitting of the absorbance values to Eq. (S6). For the calculation of ΔpH, the protonation constant (K^H) and the molar absorptivity of the protonated (ε_{HL}) and deprotonated (ε_L) methyl-orange at 506 nm was determined by recording the absorption spectra of methyl orange with *PerkinElmer Lambda 365* UV-Vis spectrophotometer in the pH range 2.5-4.5 ($[\text{methyl orange}]_{tot}$=12.5 μM, 0.15 M $NaClO_4$, 0°C). The absorbance of the methyl orange at any wavelength is a combination of the absorption of each protonated species and expressed by Eq. (S7):[14]

$$\mathrm{A} = \sum[\mathrm{H_iL}]\varepsilon_{\mathrm{H_iL}}\mathrm{l} \qquad (S7)$$

where A is the absorbance at a given wavelength, $[H_iL]$, ε_{HiL} and l are the concentration and the molar absorptivity of the species and the path length of the cell, respectively. The absorbance values (A) of methyl orange obtained at 506 nm have been fitted to the Eq (S7) (the concentration of the different protonated species have been expressed by the protonation constants K_i^H, Eq. (S1)).

III.2 Studies of the diprotonated *[Bi(H$_2$DOTP)]$^{3-}$ intermediate

In order to determine the composition and the structure of the intermediate, ΔpH is monitored by spectrophotometry in the Bi^{III} - H$_6$DOTP^{2-} reaction system ([Bi^{III}]$_{tot}$=0.5 mM, [H$_6$DOTP^{2-}], pH$_{end}$=3.17, V$_{tot}$=1.8 mL, 0.15 M NaClO$_4$, 0°C) using methyl orange as indicator. The absorption spectra of methyl orange and the absorbance values of the Bi^{3+}- H$_6$DOTP^{2-} reaction system at 506 nm as a function of time are shown in Figures S7 and S8.

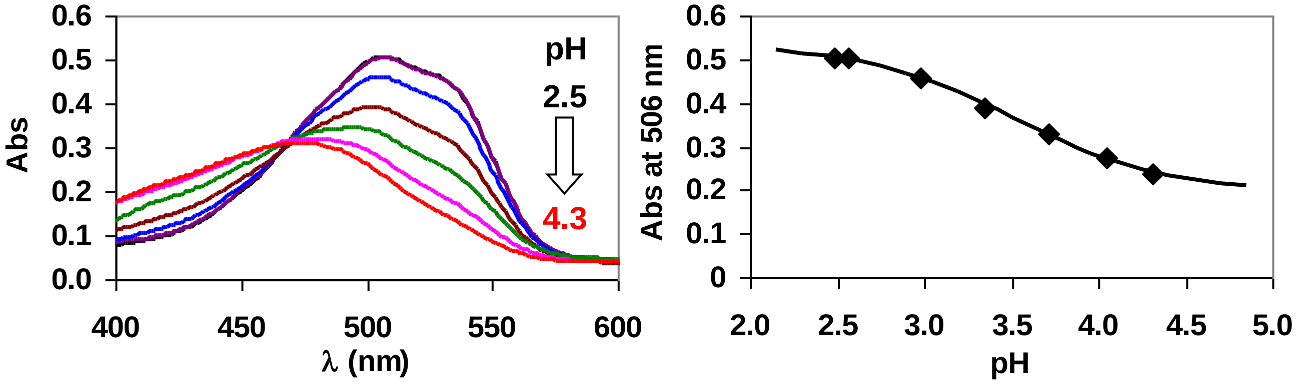

Figure S7. Absorption spectra and absorbance values at 506 nm of methyl orange ([methyl orange]$_{tot}$=12.5 μM, l=1 cm, 0.15 M NaClO$_4$, 0°C)

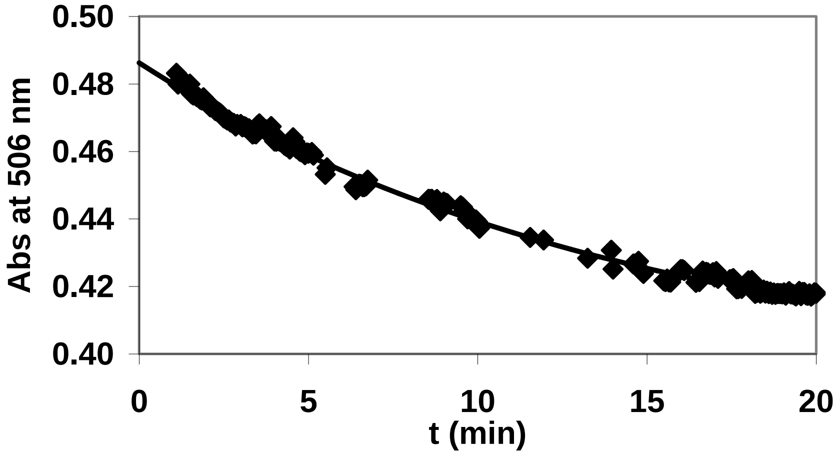

Figure S8. Absorbance values of the Bi^{III} - H$_6$DOTP^{2-} reacting system as a function of time ([Bi^{III}]$_{tot}$=0.5 mM, [H$_6$DOTP^{2-}]$_{tot}$=10 mM, [methyl orange]$_{tot}$=12.5 μM, pH$_{end}$=3.17, l=1 cm, 0.15 M NaClO$_4$, 0°C)

The absorbance values obtained at 506 nm decrease over time, which can be interpreted by the increase of the pH value in the Bi^{III}-H$_6$DOTP^{2-} reaction system (Figure S8). By taking into account the protonation constant (logK^H=3.52 (4)) and the molar absorptivity of the protonatned (HL) and deprotonated (L) methy-orange obtained at 506 nm (ε_L=15483 M^{-1}cm^{-1}; ε_{HL}=42780 M^{-1}cm^{-1}), the ΔpH is found to be +0.44 (Δ[H$^+$] = -1.2 mM) in the Bi^{III}-H_6DOTP^{2-} reaction system. Considering the large excess of H_6DOTP^{2-}, it can be assumed that the intermediate is fully formed at the beginning of the reaction. So, the increase of the pH might be accounted to the transformation of the intermediate to the final $[Bi(H_4DOTP)]^-$ complex in the H$^+$ consuming process ($[Bi(H_4DOTP)]^-$ predominates at pH$_{end}$=3.17, Table 1, Figure S6). By taking into account [Bi^{III}]$_{tot}$=0.5 mM and Δ[H$^+$] = -1.2 mM, the formation of the diprotonated $*[Bi(H_2DOTP)]^{3-}$ intermediate can be assumed in the Bi^{III}-H_6DOTP^{2-} reaction system. In $*[Bi(H_2DOTP)]^{3-}$ intermediate the Bi^{III} ion is coordinated by the four more basic phosphonate –O$^-$ donor atoms, whereas two opposite macrocyclic ring N atoms are protonated (four weakly basic deprotonated phosphonate –O$^-$ donor atoms very likely do not take place in the coordination of the Bi^{III} ion). The formation of $*[Bi(H_2DOTP)]^{3-}$ intermediate is also supported by the structural characterization of H_6DOTP^{2-} ligand (Scheme S1, Figure S2, Table S2), which reveals the availability of the more basic phosphonate –O$^-$ donor atoms for the coordination of the Bi^{III} ion, whereas four weakly basic deprotonated phosphonate –O$^-$ donor atoms might form the H-bonding with the protonated macrocyclic ring N atoms. The formation of the final in-cage Bi^{III} complex occurs by the deprotonation of the two macrocyclic ring N atoms of the diprotonated $*[Bi(H_2DOTP)]^{3-}$ intermediate, which is followed by the rearrangement to the final $[Bi(H_4DOTP)]^-$ complex with the consumption of two equivalents of H$^+$.

III.3 Formation kinetics of $[Bi(DOTA)]^-$ and $[Bi(H_xDOTP)]^{x-5}$ complexes (x=0 – 4)

The formation of $[Bi(DOTA)]^-$ and $[Bi(H_xDOTP)]^{x-5}$ complexes was followed by spectrophotometry at the absorption band of the final $[Bi(DOTA)]^-$ and $[Bi(H_xDOTP)]^{x-5}$ complexes (308 nm) in the pH range 3.0 – 6.0 (0.15 M $NaClO_4$, 25°C). The formation rates of Bi^{III} complexes have been studied under pseudo-first-order conditions that were ensured by the presence of a large excess of DOTA or DOTP ([Bi^{III}]$_{tot}$=25 μM). In these cases the rate of formation reactions can be expressed by Eq. (S8).

$$\frac{d[BiL]}{dt} = k_{obs}[Bi^{III}]_t \qquad (S8)$$

where [BiL] is the concentration of the $[Bi(DOTA)]^-$ and $[Bi(H_xDOTP)]^{x-5}$ complexes formed, [Bi^{III}]$_t$ is the total concentration of species containing Bi^{III} ions, and k_{obs} is the pseudo-first-order rate constant. The formation reaction of $[Bi(DOTA)]^-$ and $[Bi(H_xDOTP)]^{x-5}$ is investigated by varying the concentrations of ligands at different pH values. As expected, the k_{obs} vs. $[DOTA]_t$ and k_{obs} vs. $[DOTP]_t$ (Figures S9 and S10) are saturation curves indicating the fast formation of the *$[Bi(H_2DOTA)]^+$ and *$[Bi(H_2DOTP)]^{3-}$ intermediates in a pre-equilibrium characterized by a stability constant defined by Eq. (S9).

$$K_{Bi(H_2L)} = \frac{[{}^*Bi(H_2L)]}{[Bi^{III}][H_2L]} \tag{S9}$$

where [*$Bi(H_2L)$] is the concentration of *$[Bi(H_2DOTA)]^+$ and *$[Bi(H_2DOTP)]^{3-}$ intermediate, and $[H_2L]$ is the concentration of the H_2DOTA^{2-} and H_2DOTP^{6-}.

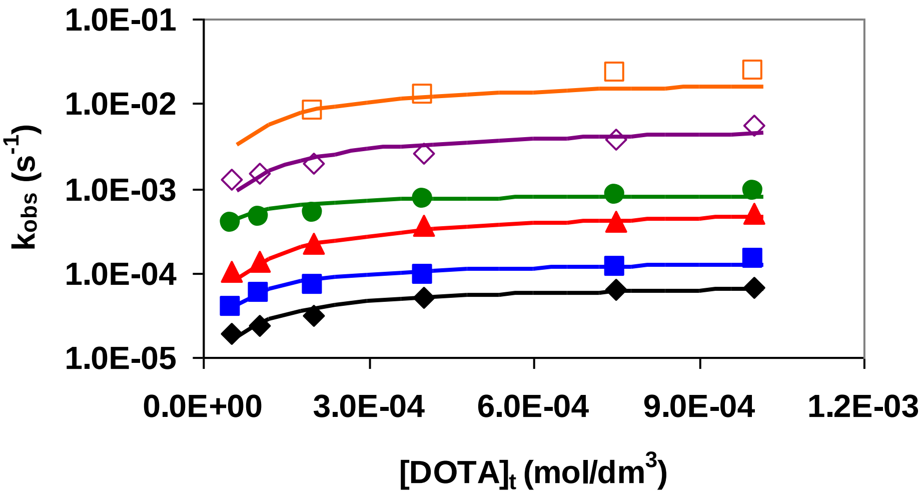

Figure S9. Pseudo-first order rate constants (k_{obs}) for the formation reaction of $[Bi(DOTA)]^-$ complex. The symbols and the solid lines represent the experimental and the calculated rate constants, respectively. ($[Bi^{III}]_{tot}$=25 μM, pH=**3.3**, **3.9**, **4.5**, **4.9**, **5.4** and **5.9**, 0.15 M $NaClO_4$, 25°C)

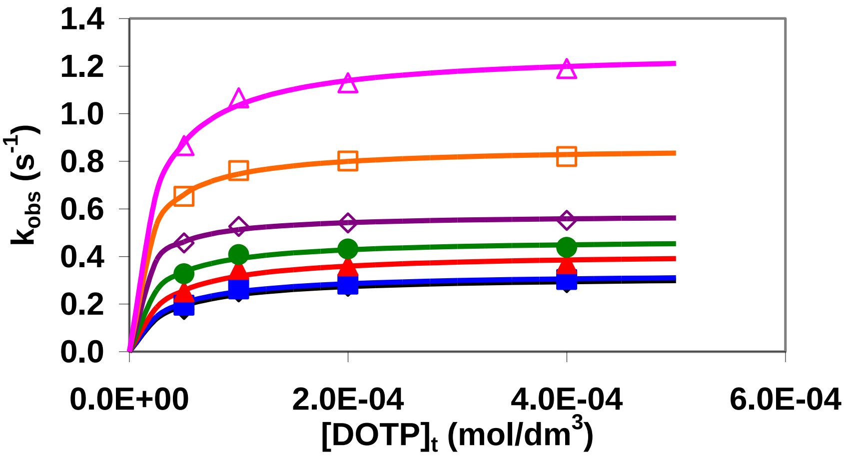

Figure S10. Pseudo-first order rate constants (k_{obs}) for the formation reaction of $[Bi(H_xDOTP)]^{x-5}$ complex. The symbols and the solid lines represent the experimental and the calculated rate constants, respectively. ($[Bi^{III}]_{tot}$=25 μM, pH=**3.0**, **3.3**, **4.0**, **4.5**, **4.8**, **5.3** and **5.6**, 0.15 M $NaClO_4$, 25°C)

The rate-determining step of the reactions is the deprotonation and rearrangement of the $*[Bi(H_2DOTA)]^+$ and $*[Bi(H_2DOTP)]^{3-}$ intermediates followed by the entrance of the metal ion into the cavity of the ligands in concentric process:

$$\frac{d[BiL]}{dt} = k_{obs}[Bi^{III}]_t = k_f[*Bi(H_2L)]_t \qquad (S10)$$

where $[*Bi(H_2L)]_t$ is the concentration of $[*Bi(H_2DOTA)]^+$ and $*[Bi(H_2DOTP)]^{3-}$ intermediates, and k_f is the rate constant characterizing the deprotonation and rearrangement of the intermediate to the final Bi^{III} complexes. The concentration of the noncomplexed ligand can be expressed by Eq. (S11) using the protonation constants of $DOTA^{4-}$ and $DOTP^{8-}$ ligand (Table S1).

$$[L]_{free}=[H_2L](1+K_3^H[H^+]+K_3^HK_4^H[H^+]^2+K_3^HK_4^HK_5^H[H^+]^3+K_3^HK_4^HK_5^HK_6^H[H^+]^4)=(1+\alpha_{2H})[H_2L] \qquad (S11)$$

where $\alpha_{2H}= K_3^H[H^+]+K_3^HK_4^H[H^+]^2+K_3^HK_4^HK_5^H[H^+]^3+K_3^HK_4^HK_5^HK_6^H[H^+]^4$. By taking into account the hydrolysis of the Bi^{III} ion the total metal ion concentration can be expressed by Eq. (S12):

$$[Bi^{III}]_t=[*Bi(H_2L)]+[Bi(OH)]+[Bi(OH)_2]+[Bi(OH)_3]+[Bi^{III}] \qquad (S12)$$

Under the experimental conditions (pH=3.0–6.0), the hydrolysis of Bi^{3+} ion may occur resulting in the formation of $[Bi(OH)]^{2+}$, $[Bi(OH)_2]^+$ and $Bi(OH)_3$ species. The formation of polymeric $Bi_x(OH)_y$ (x=6 and 9, y=12, 20 – 22) species does not take place under the experimental conditions applied in our kinetic studies.[15] Considering the hydrolysis of Bi^{III} ion, the OH^- ion may compete with the ligands for the Bi^{III} ions. By taking into account the protonation constants of $DOTA^{4-}$ and $DOTP^{8-}$ (Table S1 and Eq. (S11)), the stability constant of $[*Bi(H_2L)]$ intermediates (Eq. (S9)), the total concentration of the Bi^{III} ion (Eq. (S12)) and Eq. (S10), the pseudo-first order rate constant can be expressed by Eq. (S13).

$$k_{obs} = \frac{\dfrac{k_f K_{Bi(H_2L)}[L]_t}{1+\alpha_{2H}}}{1+\dfrac{K_{Bi(H_2L)}[L]_t}{1+\alpha_{2H}}+\alpha_{OH}} \qquad (S13)$$

where $[L]_t$ is $[DOTA]_{tot}$ and $[DOTP]_{tot}$, $\alpha_{OH}=\beta_1^{OH}/[H^+] +\beta_2^{OH}/[H^+]^2+ \beta_3^{OH}/[H^+]^3$ ($\log\beta_1^{OH}=-1.09$; $\log\beta_2^{OH}=-4.0$ and $\log\beta_3^{OH}=-8.86$ for Bi^{III} ion).[15] The pseudo-first-order rate constants determined at various pH, $[DOTA]_{tot}$ and $[DOTP]_{tot}$ values (Figures S9 and S10) are fitted to Eq. (S13) and the stability constant of the $*[Bi(H_2L)]$ intermediates (K_{MH2L}) and the k_f rate constants are calculated. The stability constants of the $*[Bi(H_2DOTA)]^+$ and $*[Bi(H_2DOTP)]^{3-}$ intermediates ($K_{Bi(H2L)}$) are presented in Table 2. The calculated k_f rate constants obtained for the formation of the $[\mathrm{Bi(DOTA)}]^-$ and $[\mathrm{Bi(H_xDOTP)}]^{x-5}$ complexes are shown in Figure S11 as a function of pH and $[\mathrm{OH^-}]$.

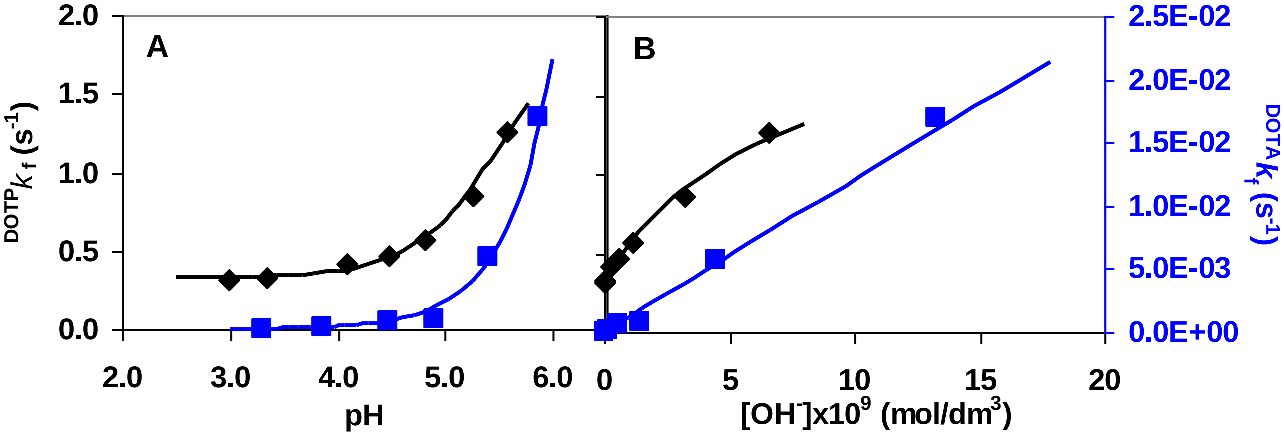

Figure S11. k_f rate constants characterize the formation of $[\mathrm{Bi(DOTA)}]^-$ (■) and $[\mathrm{Bi(H_xDOTP)}]^{x-5}$ (◆) complex as a function of pH (**A**) and $[\mathrm{OH^-}]$ (**B**). The symbols and the solid lines represent the experimental and the calculated k_f rate constants, respectively (0.15 M $\mathrm{NaClO_4}$, 25°C)

Based on the reaction mechanism proposed for the formation of $[\mathrm{M(DOTA)}]^-$ complexes with trivalent metal ions, the di- and the monoprotonated intermediates exist in equilibrium.[16–18] The dependence of the k_f values on the $[\mathrm{OH^-}]$ can be interpreted by the formation of the kinetically active monoprotonated *[Bi(HL)] intermediates via the dissociation of the diprotonated *$[\mathrm{Bi(H_2L)}]$ intermediates in an equilibrium characterized with the $K^{\mathrm{H}}_{\mathrm{Bi(HL)}}$ protonation constant (Eq. (S14)).

$$K^{\mathrm{H}}_{\mathrm{Bi(HL)}} = \frac{[\mathrm{*Bi(H_2L)}]}{[\mathrm{*Bi(HL)}][\mathrm{H^+}]} \qquad (S14)$$

The rate-controlling step of complex formation involves the $\mathrm{H_2O}$ or $\mathrm{OH^-}$ assisted deprotonation and rearrangement of the monoprotonated *[Bi(HL)] intermediates to the final [BiL] complex. However, the formation of $[\mathrm{Bi(H_xDOTP)}]^{x-5}$ might occur by the spontaneous deprotonation of the *$[\mathrm{Bi(H_2DOTP)}]^{3-}$ intermediates and rearrangement to the final $[\mathrm{Bi(H_xDOTP)}]^{x-5}$ complex at pH<4.0 (Figure S11). According to the proposed reaction mechanism, the formation rate of the $[\mathrm{Bi(DOTA)}]^-$ and $[\mathrm{Bi(H_xDOTP)}]^{x-5}$ complexes can be given by Eq. (S15).

$$\frac{\mathrm{d[BiL]}}{\mathrm{dt}} = k_{\mathrm{f}}[\mathrm{*Bi(H_2L)}]_{\mathrm{t}} = \mathrm{k}_{\mathrm{Bi(H2L)}}[\mathrm{*Bi(H_2L)}] + {}^{\mathrm{H_2O}}\mathrm{k}_{\mathrm{Bi(HL)}}[\mathrm{*Bi(HL)}] + {}^{\mathrm{OH}}\mathrm{k}_{\mathrm{Bi(HL)}}[\mathrm{*Bi(HL)}][\mathrm{OH^-}] \qquad (S15)$$

By considering the total concentration of intermediates ($[\mathrm{*Bi(H_2L)}]_{\mathrm{t}}=[\mathrm{*Bi(HL)}]+[\mathrm{*Bi(H_2L)}]$), the definition of $K^{H}_{Bi(HL)}$ protonation constant (Eq. (S14)), the k_f rate constant can be expressed by Eq. (S15).

$$k_f = \frac{k_{Bi(H2L)}K^{H}_{Bi(HL)}[H^+] + {}^{H_2O}k_{Bi(HL)} + {}^{OH}k_{Bi(HL)}K_w/[H^+]}{1 + K^{H}_{Bi(HL)}[H^+]} \qquad (S16)$$

This equation is used for the fitting of the k_f values to determine the $k_{Bi(H2L)}$, ${}^{H2O}k_{Bi(HL)}$ and ${}^{OH}k_{Bi(HL)}$ rate constants and the $K^{H}_{Bi(HL)}$ protonation constants that characterize the formation of $[Bi(DOTA)]^-$ and $[Bi(H_xDOTP)]^{x-5}$ complexes. For $[Bi(DOTA)]^-$, the protonation constants of the monoprotonated *[Bi(HL)] intermediate ($K^{H}_{Bi(HL)}$) can not be calculated, which might be explained by the very low $K^{H}_{Bi(HL)}$ due to the high affinity of Bi^{3+} ion to the ring N donor atoms. The $k_{Bi(H2L)}$, ${}^{H2O}k_{Bi(HL)}$ and ${}^{OH}k_{Bi(HL)}$ rate constants and the $K^{H}_{Bi(HL)}$ protonation constants are shown in Table 2.

To confirm the role of the general base catalysis in the deprotonation of the $*[Bi(H_2DOTA)]^+$ intermediate, the formation rate of $[Bi(DOTA)]^-$ has been followed by spectrophotometry at the absorption band of the final $[Bi(DOTA)]^-$ complex (308 nm) in the presence of acetate as general base (pH=3.3 – 5.5, 0.15 M $NaClO_4$, 25°C). The formation rates of Bi^{III} complex has been studied under pseudo-first-order conditions that is ensured by the presence of a 40-fold excess of DOTA ($[Bi^{III}]_{tot}$=25 μM, $[DOTA]_{tot}$=1.0 mM). In these cases the rate of formation reactions can be expressed by Eq. (S8). The formation reaction of $[Bi(DOTA)]^-$ has been investigated by varying the concentrations of acetate at different pH values. As expected, the k_{obs} values increase monotonously as a function of $[Ac]_t$ (Figure S12).

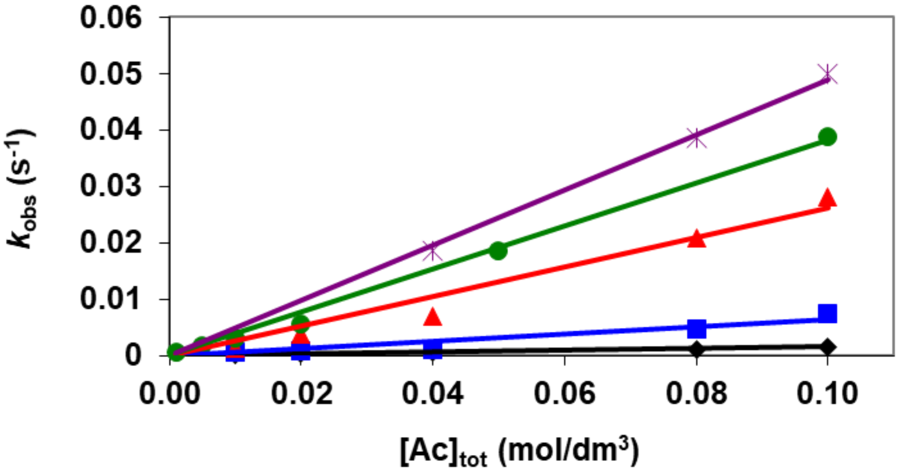

Figure S12. Pseudo-first order rate constants (k_{obs}) for the formation reaction of $[Bi(DOTA)]^-$ complex. The symbols and the solid lines represent the experimental and the calculated rate constants, respectively. ($[Bi^{III}]_{tot}$=25 μM, $[DOTA]_{tot}$=1.0 mM, pH=**3.3**, **4.0**, **4.6**, **4.8** and **5.4**, 0.15 M $NaClO_4$, 25°C).

As it is shown previously, the diprotonated *[Bi(H_2DOTA)]$^+$ intermediate is fully formed in the presence of 40 fold excess of DOTA ([Bi^{3+}]$_{tot}$=25 μM and [DOTA]$_{tot}$=1.0 mM, Figures S9). Moreover, the deprotonation of the diprotonated *[Bi(H_2DOTA)]$^+$ intermediate takes place by the formation of the monoprotonated *[Bi(HDOTA)] intermediate in our experimental condition. Since the formation rate of the Bi^{III} complexes is directly proportional to the concentration of the diprotonated *[Bi(H_2L)] intermediate (Eq. S10), it can be assumed that the rate-determining step of the reactions is the acetate as general base assisted deprotonation and rearrangement of the monoprotonated *[Bi(HDOTA)] intermediate (k'_{Ac}) followed by the entrance of the metal ion into the cavity of the DOTA^{4-}. According to the proposed reaction mechanism, the formation rate of the [Bi(DOTA)]$^-$ complex in the presence of acetate buffer can be given by Eq. (S17).

$$\frac{d[BiL]}{dt} = k_{obs}[Bi^{III}]_{tot} = k'_{Ac}\,[{*}Bi(HL)]_t\,[Ac]_{tot} \qquad (S17)$$

Under the experimental conditions and at pH between 3.3 and 5.4, the H_2O and OH$^-$ assisted deprotonation of the *[Bi(HDOTA)] intermediates is very slow process, so their contribution to the formation rate of [Bi(DOTA)]$^-$ can be neglected. By considering the total concentration of Bi^{III} ([Bi^{III}]$_{tot}$=[*Bi(HL)]$_t$) and Eq. (S17), the pseudo-first order rate constant can be expressed by Eq. (S18).

$$k_{obs} = k'_{Ac}\,[Ac]_{tot} \qquad (S18)$$

This equation is used for the fitting of the k_{obs} values in Figure S10 to determine the k'_{Ac} rate constants characterizing the acetate anion assisted formation of [Bi(DOTA)]$^-$ complexes at given pH. The k'_{Ac} rate constants as a function of pH are shown in Figure S13.

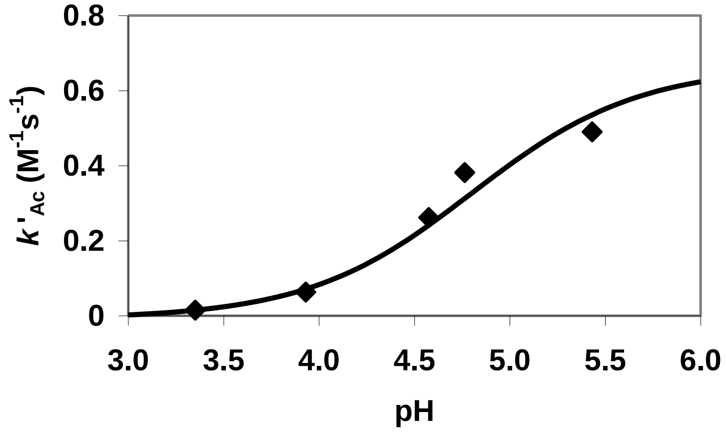

Figure S13. k'_{Ac} rate constants characterizes the acetate assisted deprotonation and transformation of the *[Bi(HDOTA)] intermediate to the final [Bi(DOTA)]$^-$ complex The symbols and the solid lines represent the experimental and the calculated rate constants, respectively. (0.15 M $NaClO_4$, 25°C).

The k'_{Ac} rate constants increase with the increase of the pH. The dependence of the k'_{Ac} values on the pH can be interpreted by the formation of the kinetically active deprotonated acetate anion, which might assist as general base the deprotonation *[Bi(HDOTA)] intermediate via proton exchange processes. By considering the total concentration of acetate ($[Ac]_{tot}=[HAc]+[Ac^-]$), the definition of protonation constant of the acetate anion (Eq. (S1), the k'_{Ac} rate constant can be expressed by Eq. (S19).

$$k'_{Ac} = \frac{k_{Ac}}{1 + {}^{Ac}K_1^H[H^+]} \qquad (S19)$$

where k_{Ac} is the rate constant characterizing the acetate anion assisted deprotonation of *[Bi(HDOTA)] intermediate, whereas ${}^{Ac}K_1^H$ is the protonation constant of the acetate anion. This equation is used for the fitting of the k'_{Ac} values to determine the k_{Ac} rate constant and the ${}^{Ac}K_1^H$ protonation constant of the acetate anion. The protonation constant of the acetate anion obtained by the fitting of the kinetic data at Figures S13 is $\log{}^{Ac}K_1^H$= 4.8 (2), which is in agreement with that of the acetate anion published for the same condition in the literature ($\log{}^{Ac}K_1^H$= 4.52, 25°C, 0.15 M $NaClO_4$).[19] The k_{Ac} rate constants characterizing the acetate assisted deprotonation and transformation of *[Bi(HDOTA)] intermediate to the final $[Bi(DOTA)]^-$ complex is found to be $k_{Ac} = 0.7 \pm 0.1\ M^{-1}s^{-1}$.

III.4 Formation kinetics of $[Bi(DOTA)]^-$ and $[Bi(H_xDOTP)]^{x-5}$ complexes in the presence of citrate (x=0 – 4)

The effect of citrate on the formation rate of $[Bi(DOTA)]^-$ and $[Bi(H_xDOTP)]^{x-5}$ complexes has been followed by spectrophotometry at the absorption band of the final $[Bi(DOTA)]^-$ and $[Bi(H_xDOTP)]^{x-5}$ complexes (308 nm) in the presence of 0.25 – 2.0 mM citrate (pH=3.0 – 5.6, 0.15 M $NaClO_4$, 25°C). Some characteristic absorption spectra of the Bi^{III} - DOTA – citrate reacting system are shown in Figure S14.

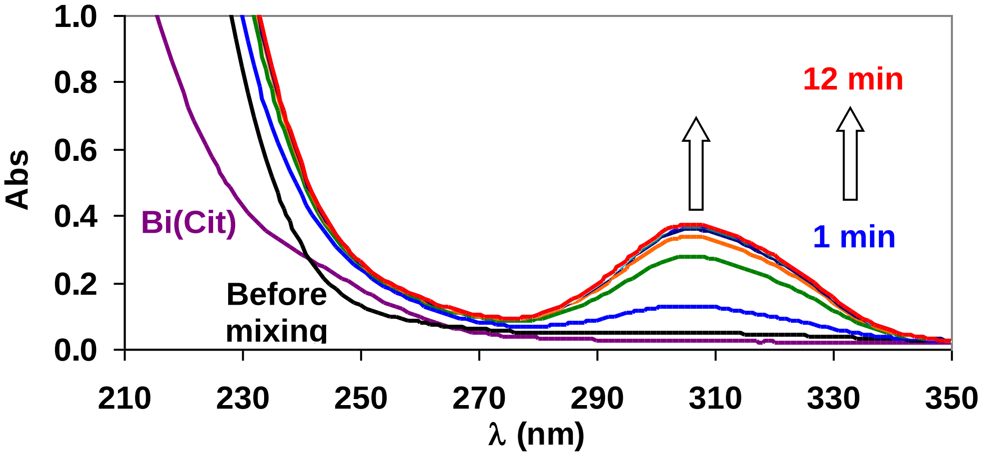

Figure S14. Absorption spectra of Bi^{III}-DOTA-citrate reacting system ($[Bi^{III}]_{tot}$=50 μM, $[DOTA]_{tot}$=2.0 mM, $[Cit]_{tot}$=4.0 mM; pH=4.0, 0.15 M $NaClO_4$, 25°C) l =1 cm

The formation reaction of $[Bi(DOTA)]^-$ and $[Bi(H_xDOTP)]^{x-5}$ has been investigated by varying the concentrations of citrate between 0.25 – 2.0 mM at different pH values in the presence of ligand excess guaranteeing the pseudo-first-order kinetic condition ($[Bi^{III}]_{tot}$=25 μM, $[DOTA]_{tot}$=1.0 mM, $[DOTP]_{tot}$=0.1 mM). The k_{obs} vs. $[Cit]_t$ for the formation of $[Bi(DOTA)]^-$ and $[Bi(H_xDOTP)]^{x-5}$ are shown in Figures S15 and S16.

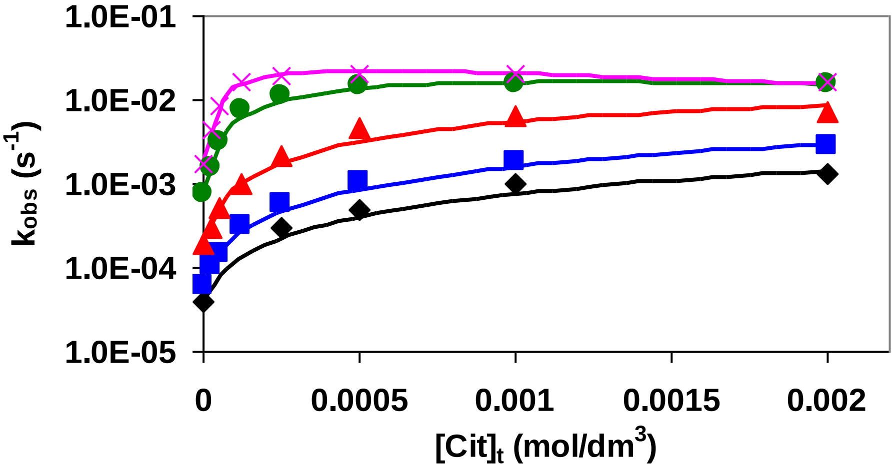

Figure S15. Pseudo-first order rate constants (k_{obs}) for the formation reaction of $[Bi(DOTA)]^-$ complex in the presence of citrate at different pH. The symbols and the solid lines represent the experimental and the calculated rate constants, respectively. ($[Bi^{III}]_{tot}$=25 μM, $[DOTA]_{tot}$=1.0 mM, pH=**3.0**, **3.4**, **4.0**, **4.6** and **5.0**, 0.15 M $NaClO_4$, 25°C)

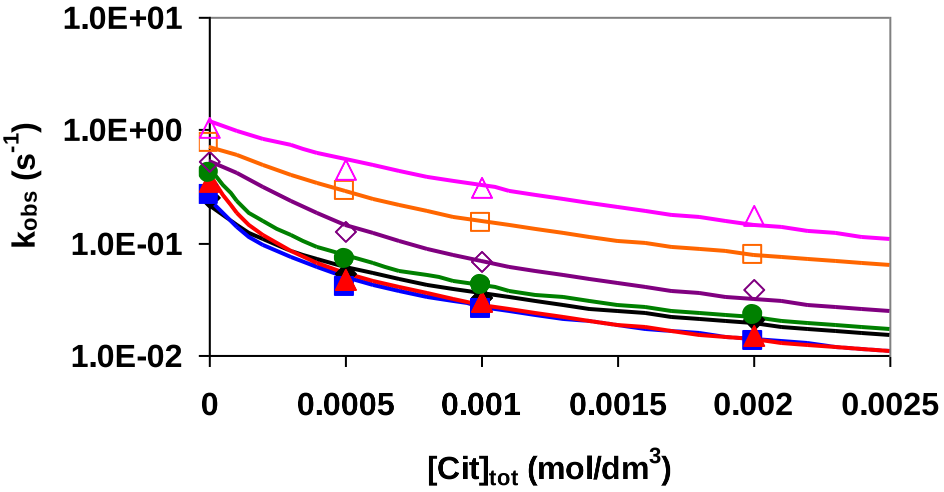

Figure S16. Pseudo-first order rate constants (k_{obs}) for the formation reaction of $[Bi(H_xDOTP)]^{x-5}$ complex in the presence of citrate at different pH. The symbols and the solid lines represent the experimental and the calculated rate constants, respectively. ($[Bi^{III}]_{tot}$=25 μM, $[DOTP]_{tot}$=0.1 mM, pH=**3.0**, **3.3**, **4.0**, **4.5**, **4.8**, **5.3** and **5.6**, 0.15 M $NaClO_4$, 25°C)

Interestingly, the formation rate (k_{obs}) of $[Bi(DOTA)]^-$ increase with the citrate concentration showing the saturation curve (Figure S15). However, the k_{obs} values characterize the formation of the $[Bi(H_xDOTP)]^{x-5}$ decreases with the increase of $[Cit]_t$ (Figure S16). The comparison of the absolute values of the k_{obs} reaction rate constants obtained in the absence and presence of 2.0 mM citrate indicates that citrate accelerates the formation of $[Bi(DOTA)]^-$ by a factor of 8 - 10 in the pH range pH 3.0-5.0. The presence of 2.0 mM citrate slows down the formation of $[Bi(H_xDOTP)]^{x-5}$ by a factor of 10 at pH between 3.0 and 4.5, and by about 5 times in the pH range 4.8-5.6. Under the experimental conditions and at pH between 3.0 and 5.6, the Bi^{III} ion might form [Bi(Cit)] and $[Bi(Cit)_2]^{3-}$ complexes characterized by Eqs. (S20) and (S21) ($\log K_{Bi(Cit)}$=10.78, $\log K_{Bi(Cit)2}$=5.05, 37°C, 0.15 M $NaClO_4$).[20]

$$Bi^{III} + Cit^{3-} \overset{K_{Bi(Cit)}}{\rightleftharpoons} Bi(Cit) \qquad (S20)$$

$$Bi(Cit) + Cit^{3-} \overset{K_{Bi(Cit)2}}{\rightleftharpoons} Bi(Cit)_2 \qquad (S21)$$

As it has been shown previously, the diprotonated *$[Bi(H_2L)]$ intermediate is fully formed in the presence of ligand excess ($[Bi^{3+}]_{tot}$=25 μM, $[DOTA]_{tot}$=1.0 mM and $[DOTP]_{tot}$=0.1 mM, Figures S9 and S10). Since the formation rate of the Bi^{III} complexes is directly proportional to the concentration of the diprotonated *$[Bi(H_2L)]$ intermediate (Eq. S10), it can be assumed that the slower formation of $[Bi(H_xDOTP)]^{x-5}$ in the presence of citrate is caused by the formation of [Bi(Cit)] and $[Bi(Cit)_2]^{3-}$ complexes, which decreases the concentration of the kinetically active diprotonated $*[Bi(H_2DOTP)]^{3-}$ intermediate. To explain the faster formation of $[Bi(DOTA)]^-$ in the presence of citrate, we hypothesize the intermediate contains a citrate ligand coordinated to the Bi^{III} ion ($*[Bi(H_2DOTA)(citrate)]^{2-}$, Eq. (S22)), which deprotonates and transforms to the final $[Bi(DOTA)]^-$ complex in the rate determining step. The rate determining deprotonation and transformation of the $*[Bi(H_2DOTA)(citrate)]^{2-}$) intermediate takes place simultaneously with release of the coordinated citrate ligand. The formation of similar ternary $*[Ga(HNOTA)(citrate)]^{2-}$ intermediate has been found in the Ga(citrate) – NOTA reacting system.[21]

$$\mathrm{Bi(Cit)} + \mathrm{H_2L} \overset{\mathrm{K_{Bi(H2L)(Cit)}}}{\rightleftharpoons} \mathrm{Bi(H_2L)(Cit)} \tag{S22}$$

$$\mathrm{K_{Bi(H_2L)(Cit)}} = \frac{[\mathrm{Bi(H_2L)(Cit)}]}{[\mathrm{Bi(Cit)}][\mathrm{H_2L}]}$$

The formation rates of Bi^{III}-complexes have been studied under pseudo-first-order conditions that is ensured by the presence of a large excess of ligands ($[Bi^{III}]_{tot}$=25 μM, $[DOTA]_{tot}$=1.0 mM and $[DOTP]_{tot}$=0.1 mM). In these conditions the rate of formation reactions can be expressed by Eq. (S8). The rate-determining step of the reactions is the deprotonation and rearrangement of the $*[Bi(H_2DOTA)]^+$ and $*[Bi(H_2DOTA)(citrate)]^{2-}$ intermediates followed by the entrance of the metal ion into the cavity of the DOTA ligand:

$$\frac{\mathrm{d[BiL]}}{\mathrm{dt}} = k_{\mathrm{obs}}[\mathrm{Bi}^{3+}]_{\mathrm{t}} = \mathrm{k_{Bi(H2L)}[Bi(H_2L)]} + {}^{\mathrm{H_2O}}\mathrm{k_{Bi(HL)}[Bi(HL)]} + {}^{\mathrm{HO}}\mathrm{k_{Bi(HL)}[Bi(HL)]} + \mathrm{k_{Bi(Cit)(H2L)}[Bi(H_2L)(Cit)]} \tag{S23}$$

where $[*Bi(H_2L)]$, $[*Bi(HL)]$ and $[*Bi(H_2L)(Cit)]$ is the concentration of $*[Bi(H_2L)]$, $*[Bi(HL)]$ and $*[Bi(H_2L)(citrate)]$) intermediates. $k_{Bi(H2L)(Cit)}$ and $k_{Bi(H2L)}$ are the rate constants characterizing the spontaneous deprotonation and rearrangement of the $*[Bi(H_2L)(citrate)]$ and $*[Bi(H_2L)]$ intermediate, whereas ${}^{H2O}k_{Bi(HL)}$ and ${}^{OH}k_{Bi(HL)}$ are the rate constants characterizing H_2O and OH^- assisted deprotonation and rearrangement of the $*[Bi(HL)]$ intermediate. The concentration of the noncomplexed citrate can be expressed by Eq. (S24).

$$[\mathrm{Cit}]_{\mathrm{f}}=[\mathrm{Cit}](1+{}^{\mathrm{cit}}K_1^{\mathrm{H}}[\mathrm{H}^+]+{}^{\mathrm{cit}}K_1^{\mathrm{H}}\,{}^{\mathrm{cit}}K_2^{\mathrm{H}}[\mathrm{H}^+]^2+{}^{\mathrm{cit}}K_1^{\mathrm{H}}\,{}^{\mathrm{cit}}K_2^{\mathrm{H}}\,{}^{\mathrm{cit}}K_3^{\mathrm{H}}[\mathrm{H}^+]^3)=(1+\alpha_{\mathrm{Cit}})[\mathrm{Cit}] \tag{S24}$$

where ${}^{cit}K_1^H$=5.58 (1), ${}^{cit}K_2^H$=4.33 (2), ${}^{cit}K_3^H$=2.93 (2) (0.15 M $NaClO_4$, 25°C) are the corresponding protonation constants citrate, whereas α_{Cit}= ${}^{cit}K_1^H[H^+]+{}^{cit}K_1^H\,{}^{cit}K_2^H[H^+]^2+{}^{cit}K_1^H$

${}^{cit}K_2^H\,{}^{cit}K_3^H[H^+]^3$. By taking into account the concentration of the noncomplexed H_2L ligand and citrate (Eqs. (S11) and (S24)), stability constants of [Bi(Cit)] and $[Bi(Cit)_2]^{3-}$ complexes and $*[Bi(H_2L)(citrate)]$) intermediates ((Eqs. (S20) - (S21)) and the hydrolysis of the Bi^{III} ion (Eq. (S12)), the total metal ion concentration can be expressed by Eq. (S25):

$$[Bi^{III}]_t=[*Bi(H_2L)]+[*Bi(HL)]+[Bi(Cit)]+[Bi(Cit)_2]+[Bi(Cit)(H_2L)]+[Bi(OH)]+[Bi(OH)_2]+ \\ +[Bi(OH)_3]+[Bi^{III}])=[Bi^{III}]\times\gamma \qquad (S25)$$

$$\gamma=\left(1+\frac{K^*_{Bi(H_2L)}[L]_{tot}}{1+\alpha_{2H}}+\frac{\dfrac{K^*_{Bi(H_2L)}[L]_{tot}}{(1+\alpha_{2H})}}{K^H_{Bi(HL)}[H^+]}+\frac{K_{Bi(Cit)}[Cit]_{tot}}{1+\alpha_{cit}}+K_{Bi(Cit)}K_{Bi(Cit)_2}\left(\frac{[Cit]_{tot}}{1+\alpha_{cit}}\right)^2+\frac{K^*_{Bi(H_2L)(Cit)}K_{Bi(Cit)}[L]_{tot}}{(1+\alpha_{2H})}\times\frac{[Cit]_{tot}}{(1+\alpha_{cit})}+\alpha_{OH}\right)$$

By taking into account the concentration of the noncomplexed H_2L ligand and citrate (Eqs. (S11) and (S24)), the stability constant of $*[Bi(H_2L)]$ and $*[Bi(H_2L)(citrate)]$) intermediates (Eqs. (S9) and (S22)), the definition of $K^H_{Bi(HL)}$ protonation constant (Eq. (S14)), the total concentration of the Bi^{III} ion (Eq. (S25)) and Eq. (S23), the pseudo-first order rate constant can be expressed by Eq. (S26).

$$k_{obs}=\left[\frac{k_{Bi(H2L)}K^*_{Bi(H_2L)}[L]_t}{1+\alpha_{2H}}+\frac{\dfrac{{}^{H_2O}k_{Bi(HL)}K^*_{Bi(H_2L)}[L]_t}{1+\alpha_{2H}}}{K^H_{Bi(HL)}[H^+]}+\frac{\dfrac{{}^{OH}k_{Bi(HL)}K^*_{Bi(H_2L)}[L]_t[OH]}{1+\alpha_{2H}}}{K^H_{Bi(HL)}[H^+]}+\frac{k_{Bi(Cit)(H_2L)}K^*_{Bi(H_2L)(Cit)}K_{Bi(Cit)}[L]_{tot}}{1+\alpha_{2H}}\times\frac{[Cit]_{tot}}{(1+\alpha_{cit})}\right]\times\frac{1}{\gamma} \qquad (S26)$$

Eq. (S26) was used for the fitting of the k_{obs} values at Figures S15 and S16. In the fitting procedure of the kinetic data of the formation of $[Bi(H_xDOTP)]^{x-5}$ and $[Bi(DOTA)]^-$, the $k_{Bi(H2L)(Cit)}$ rate constant characterizing the deprotonation and transformation of $*[Bi(H_2DOTA)(citrate)]^{2-}$ intermediate, the stability constant of $*[Bi(H_2DOTA)(citrate)]^{2-}$ intermediate and Bi(Cit) complex were calculated, whereas the $\log K_{Bi(Cit)2}$ was fixed ($\log K_{Bi(Cit)2}$=5.05, 37°C, 0.15 M $NaClO_4$).[20] The formation of the $*[Bi(H_2L)(citrate)]$) intermediate has been neglected in the Bi^{III} - DOTP – citrate reacting system. The stability constant of the $*[Bi(H_2DOTP)]^{2-}$ intermediate, the $k_{Bi(H2L)}$, ${}^{H2O}k_{Bi(HL)}$ and ${}^{OH}k_{Bi(HL)}$ rate constants and the $K^H_{Bi(HL)}$ protonation constants that characterize the formation of $[Bi(DOTA)]^-$ and $[Bi(H_xDOTP)]^{x-5}$ complexes obtained in the absence of citrate were fixed in the calculations. The stability constant of the Bi(Cit) complex obtained by the fitting of the kinetic data at Figures S15 and S16 were $\log K_{Bi(Cit)}$= 11.55 (8) and 11.08 (6), which were in agreement with the stability constant of Bi(Cit) complex published in the literature

($\log K_{Bi(Cit)}$=10.78, 37°C, 0.15 M $NaClO_4$).[20] The stability constant of the *$[Bi(H_2DOTA)(citrate)]^{2-}$ intermediate was found to be $\log K_{Bi(H2L)(Cit)}$=4.5 (1) ($\log \beta_{Bi(H2L)(Cit)}$=[$Bi(H_2DOTA)(citrate)$]/[$Bi^{III}$][$H_2DOTA$][citrate]=16.1), which is very similar to that of *$[Ga(HNOTA)(citrate)]^{2-}$ intermediate ($\log \beta_{Ga(HNOTA)(Cit)}$=14.9 – 16.7).[21] The $k_{Bi(H2L)(cit)}$ rate constants characterizing the deprotonation and transformation of *[$Bi(H_2DOTA)(citrate)$] intermediate to the final $[Bi(DOTA)]^-$ complex are shown in Figure S17.

The variation of the $k_{Bi(H2L)(cit)}$ values as a function pH (Figure S17) shows an unusual pH dependency. We assume that the final $[Bi(DOTA)]^-$ complex from *$[Bi(H_2DOTA)(citrate)]^{2-}$ occurs by protonation and dissociation of the coordinated citrate ($Hcitrate^{2-}$ and $H_2citrate^-$ species prevail at pH 3.0–5.6), followed by deprotonation of ring nitrogen atoms and transformation of the intermediate to the final Bi^{III}-complex. These processes might occur simultaneously or consecutively. Protonation of the citrate ligand might be assisted by H^+ (k_1 and k_2), while the deprotonation of the ring N donor atoms occurs via the assistance of H_2O and OH^- (characterized by k_0 and k_3 rate constants).

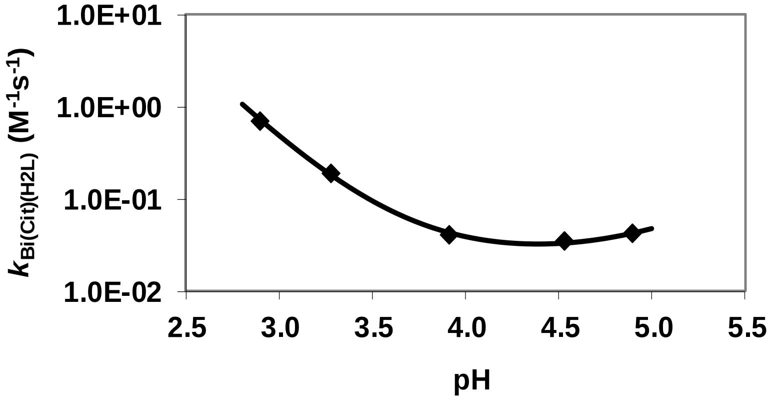

Figure S17. $k_{Bi(Cit)(H2L)}$ rate constants characterizing the transformation of the *$[Bi(H_2DOTA)(citrate)]^{2-}$ intermediate to the final $[Bi(DOTA)]^-$ complex, respectively. The symbols and the solid lines represent the experimental and the calculated rate constants, respectively. (0.15 M $NaClO_4$, 25°C)

Inspection of the pH-dependency of $k_{Bi(H2L)(cit)}$ values (shown in Figure S17) confirms that the assistance of H^+ dominates below pH=4, whereas the H_2O and OH^- assisted pathways has an important role in the formation of $[Bi(DOTA)]^-$ above pH=4. Taking into account the possible pathways for the transformation of the *$[Bi(H_2DOTA)(citrate)]^{2-}$ intermediate to the final $[Bi(DOTA)]^-$, the $k_{Bi(H2L)(cit)}$ rate constant can be expressed by Eq (S27).

$$k_{Bi(H2L)(cit)} = k_0 + k_1[H^+] + k_2[H^+]^2 + k_3[OH^-] \quad (S27)$$

The rate constants characterizing the H_2O, H^+ and OH^- assisted transformation of the *$[Bi(H_2DOTA)(citrate)]^{2-}$ intermediate to the final $[Bi(DOTA)]^-$ are k_0=(2.0 ± 0.7)×10^{-2} s^{-1}, k_1= 13 ± 6 $M^{-1}s^{-1}$, k_2= (3.3 ± 0.7) ×10^5 $M^{-1}s^{-1}$ and k_3= (1.5 ± 0.6) ×10^7 $M^{-1}s^{-1}$, respectively. Comparison of the ${}^{H2O}k_{Bi(HL)}$ = 2 ± 1)×10^{-5} s^{-1} and ${}^{HO}k_{Bi(HL)}$= 1.2±0.2) ×10^6 $M^{-1}s^{-1}$ values (characterizing the H_2O and OH^- assisted transformation of the monoprotonated *[Bi(HDOTA)] intermediate) with those values characteristic for the *$[Bi(H_2DOTA)(citrate)]^{2-}$ intermediate (k_0=(2.0 ± 0.7) ×10^{-2} s^{-1} and k_3= (1.5 ± 0.6) ×10^7 $M^{-1}s^{-1}$) supports that the faster formation of $[Bi(DOTA)]^-$ in the presence of citrate auxiliary ligand might be contributed to the faster H_2O and OH^- assisted transformation of the *$[Bi(H_2DOTA)(citrate)]^{2-}$ intermediate at pH>4.0.

III.5 Formation kinetics of $[Bi(DOTA)]^-$ complex in the presence of citrate, acetate and MES buffers.

The effect of acetate and MES buffer for the formation rate of $[Bi(DOTA)]^-$ complex was investigated by spectrophotometry at the absorption band of the final $[Bi(DOTA)]^-$ and complex (308 nm) in the presence of 0.25 mM citrate ($[Bi^{3+}]_{tot}$=25 µM, $[DOTA]_{tot}$=1.0 mM, pH=5.0, 0.15 M $NaClO_4$, 25°C). The k_{obs} vs. $[Ac]_t$ and k_{obs} vs. $[MES]_t$ for the formation of $[Bi(DOTA)]^-$ are shown in Figures S18 and S19.

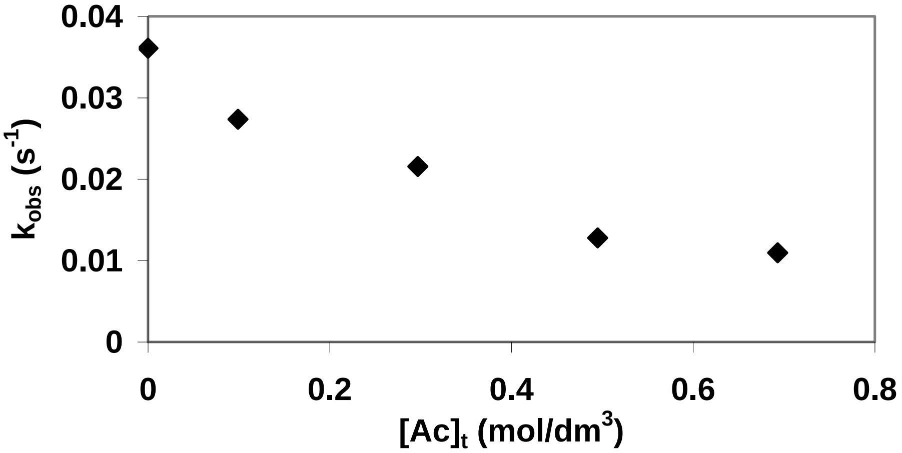

Figure S18. Pseudo-first order rate constants (k_{obs}) for the formation reaction of $[Bi(DOTA)]^-$ complex in the presence of acetate buffer. ($[Bi^{III}]_{tot}$=25 µM, $[DOTA]_{tot}$=1.0 mM, $[citrate]_{tot}$=0.25 mM pH= 5.0, 0.15 M $NaClO_4$, 25°C)

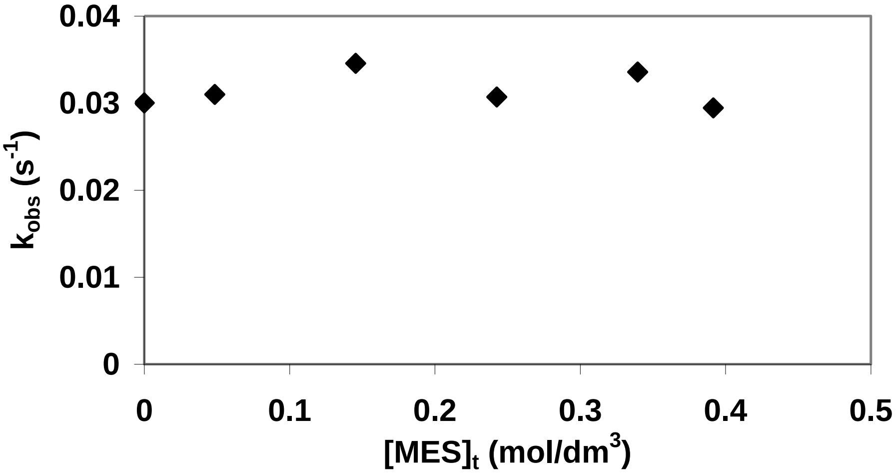

Figure S19. Pseudo-first order rate constants (k_{obs}) for the formation reaction of $[Bi(DOTA)]^-$ complex in the presence of MES buffer. ($[Bi^{III}]_{tot}$=25 μM, $[DOTA]_{tot}$=1.0 mM, $[citrate]_{tot}$=0.25 mM pH= 5.0, 0.15 M $NaClO_4$, 25°C)

IV. Dissociation kinetic studies of $[Bi(DOTA)]^-$ and $[Bi(H_4DOTP)]^-$ complexes.

IV.1 Experimental

The kinetic inertness of the $[Bi(DOTA)]^-$ and $[Bi(H_4DOTP)]^-$ was characterized by the rates of the transchelation reactions taking place with H_4AAZTA ligand. The exchange reactions were studied by spectrophotometry, following the dissociation of the $[Bi(DOTA)]^-$ and $[Bi(H_4DOTP)]^-$ complexes at 308 nm with *PerkinElmer Lambda 365* UV-Vis spectrophotometer. The concentration of the Bi^{III}-complex was 50 μM, while the concentration of H_4AAZTA was 40-fold higher to ensure pseudo-first-order conditions. The temperature was maintained at 25°C and the ionic strength of the solutions was kept constant, 0.15 M for $NaClO_4$. The exchange rates were studied in the pH range of 1.0 – 3.3. For keeping the pH values constant, mono-chloroacetic acid buffer (0.01 M) was used. The pseudo-first-order rate constants (k_{obs}=k_d) were calculated by fitting the absorbance data to Eq. (S6). Calculation of the kinetic parameters were performed by the fitting of the absorbance - time data pairs to Eq. (S6) with the *Micromath Scientist* computer program (version 2.0, Salt Lake City, UT, USA).

The ligand exchange reaction of $[Bi(DOTA)]^-$ and $[Bi(DOTP)]^{5-}$ with HP-DO3A^{3-} as an exchanging ligand have also been studied by *Capillary Zone Electrophoresis* (CZE) in the pH range of 10.0 – 12.0. The transchelation reactions of $[Bi(DOTA)]^-$ and $[Bi(DOTP)]^{5-}$ were studied by following the formation of the [Bi(HP-DO3A)] complex (migration time is 5.2 min) with *Agilent 7100 Capillary Electrophoresis* system. The concentration of the HP-DO3A was 5 and 10 mM, while the Bi^{III}-complexes was employed in high excess ($[BiL]_{tot}$=60 mM), in order to guarantee pseudo-first-order conditions. The temperature was maintained at 25°C and the ionic strength of the solutions was kept constant, 0.15 M for $NaClO_4$. The exchange rates were studied in the pH range about 9.0 – 11.5. For keeping the pH values constant, 0.01 M phosphate buffers were used.

The rates of the transchelation reactions have been studied in the presence of excess of the Bi^{III}-complexes, when the reactions can be regarded as pseudo-first-order ones and the rates of transmetallation can be expressed by Eq. (S28):

$$-\frac{d[\mathrm{BiL}]_t}{dt} = \frac{d[\mathrm{Bi(HP\text{-}DO3A)}]_t}{dt} = k_d[\mathrm{BiL}]_t \qquad (S28)$$

where k_d is a pseudo-first-order rate constant, $[BiL]_t$ and $[Bi(HP\text{-}DO3A)]_t$ are the concentration of complexes, containing the species $[Bi(DOTA)]^-$, $[Bi(DOTP)]^{5-}$ and [Bi(HP-DO3A)] at the time *t*, respectively. During the progress of the transchelation reaction the concentration of the [Bi(HP-DO3A)] complex increases. Following the signal of the [Bi(HP-DO3A)] formed in transchelation reaction of the Bi^{III}-complexes, the first-order rate constant, k_d can be expressed by Eq. (S29):

$$k_d = \frac{\Delta\int}{\Delta t} \times \frac{1}{\int^{M}_{\mathrm{Bi(HP-DO3A)}}} \times \frac{1}{[\mathrm{BiL}]_t} \qquad (S29)$$

In the Eq. (S29) $\Delta\int$ is the increase of the integral value of [Bi(HP-DO3A)] during the time Δt. $\int^{M}_{Bi(HP\text{-}DO3A)}$ is the molar integral value of the [Bi(HP-DO3A)] ($\int^{M}_{Bi(HP\text{-}DO3A)}=1.96\times10^{6}$ $mAU^{-1}M^{-1}$), which was determined by recording the CZE electropherograms of 0.2, 0.4, 0.6, 0.8, 1.0, 1.2, 1.4 and 1.7 mM solutions of [Bi(HP-DO3A)] complex at pH=7.4 and 25°C in the presence of 0.15 M $NaClO_4$ ionic strength.

CZE separations were performed with *Agilent 7100 Capillary Electrophoresis* system using bare fused-silica capillaries of 64 cm x 50 μm i.d. (*Agilent*). Before the first use, the capillary was washed with 1.0 M NaOH (15 min), with 0.1 M NaOH (30 min) and with the buffer electrolyte (30 min). Prior to CE analysis all buffers were filtered through a 0.45 μm syringe filter and stored in refrigerator at +4ºC. In CZE the sample solutions were introduced at the anodic end of the capillary in normal mode (50 mbar, 20 s). The effective length of the capillary was 56 cm. The capillary was preconditioned with the buffer electrolyte (50 mM sodium tetraborate, pH=9.0) for 3 minutes. The separation was performed at 25°C with the application of 20 kV voltage. After analysis, the postconditioning (0.1 M NaOH (3 min) and buffer (3 min)) was applied to remove all possibly adsorbed materials from the capillary. In all measurements, 5 mM DMSO as internal standard was applied to correct the migration time of components on the electropherogram. The detection was carried out by on-column DAD measurement at 195 nm. The electropherograms were recorded and processed by *ChemStation* computer program of B.04.02 version (*Agilent*).

IV.2 Transchelation reactions of $[Bi(DOTA)]^-$ and $[Bi(H_4DOTP)]^-$ complexes with H_4AAZTA ligand

The rates of the transchelation reactions (Eq. (S30)) between Bi^{III} complexes and H_4AAZTA were studied by spectrophotometry at acidic condition on the absorption band of the Bi^{III} complexes (308 nm) in the presence of 40 fold H_4AAZTA excess ($[Bi(DOTA)]_{tot}=[Bi(DOTP)]_{tot}=50$ μM, $[AAZTA]_{tot}= 2.0$ mM, pH=1.0 – 3.3, 0.15 M $NaClO_4$, 25°C).

$$\mathrm{BiL} + \mathrm{AAZTA} \rightleftharpoons \mathrm{Bi(AAZTA)} + \mathrm{L} \qquad (\mathrm{L=DOTA,\ DOTP}) \qquad \textit{(S30)}$$

In the presence of excess of the exchanging ligand, the transchelation can be treated as a pseudo-first-order process and the rate of reactions can be expressed with the Eq. (S31), where k_d is a pseudo-first-order rate constant, and $[BiL]_t$ is the total concentration of the Bi^{III} complexes.

$$-\frac{d[\mathrm{BiL}]_t}{dt} = k_d[\mathrm{BiL}]_t \qquad \textit{(S31)}$$

The rates of the transmetallation reactions have been studied in the pH range of 1.0 – 3.3. The obtained pseudo-first order rate constants k_d are presented in Figure S20 as a function of pH and $[H^+]$.

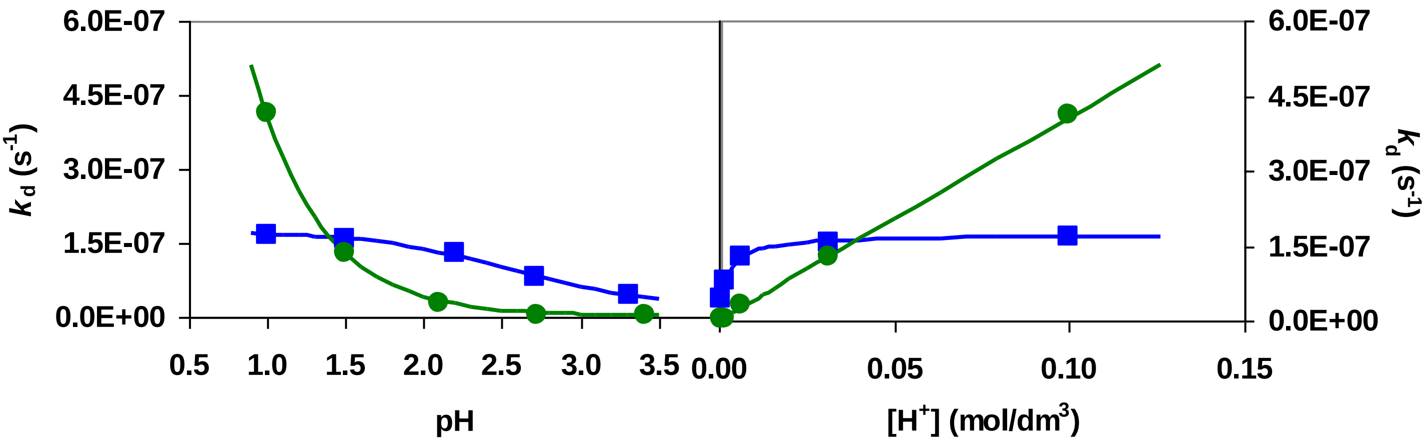

Figure S20. k_d pseudo-first-order rate constant characterizing the transchelation reactions of **$[Bi(DOTA)]^-$** and **$[Bi(H_4DOTP)]^-$** with H_4AAZTA ligand. The solid lines and the symbols represent the calculated and measured k_d rate constants. ($[Bi(DOTA)]^-_{tot}$ = $[Bi(DOTP)]^{5-}_{tot}$ =50 μM, $[AAZTA]_{tot}$=2.0 mM, $[CA]_{tot}$=0.01 M, 0.15 M $NaClO_4$, 25°C).

The kinetic data presented in Figure S20 show that the k_d values increase with increasing H^+ ion concentration. On the basis of literature data,[22] the rate-determining step of the transchelation reactions is the dissociation of the Gd^{III} complexes with DOTA derivatives, followed by the fast reaction between the free Gd^{III} ion and the exchanging ligand or by the rapid reaction between the free chelate and the exchanging metal ion. The exchanging metal ions or ligand do not take place directly in the transmetallation or transchelation reactions.[22–25] By taking into account the speciation of Bi^{III} - DOTA and Bi^{III} - DOTP systems (Table 1), the dependence of the k_d values on pH and $[H^+]$ (Figure S20) can be interpreted as spontaneous (${}^{dis}k_0$, Eq. (S32)) and H^+-ion assisted dissociation (${}^{dis}k_H$, Eq. (S34)) of Bi^{III}-complexes via the formation of [Bi(HDOTA)] and $[Bi(H_5DOTP)]$ intermediates (K^H_{BiL}, Eq. (S33)) in the investigated pH ranges.

$$\mathrm{BiL} \xrightarrow{{}^{dis}k_0} \mathrm{Bi} + \mathrm{L} \qquad (S32)$$

$$\mathrm{BiL} + \mathrm{H}^+ \overset{K^{H}_{BiL}}{\rightleftharpoons} {}^*\mathrm{Bi(HL)} \qquad (S33)$$

$$K^{H}_{BiL} = \frac{[\mathrm{Bi(HL)}]}{[\mathrm{BiL}][\mathrm{H}^+]}$$

$$ {}^*\mathrm{Bi(HL)} \xrightarrow{{}^{dis}k_H} \mathrm{Bi}^{3+} + \mathrm{HL} \qquad (S34)$$

where *[Bi(HL)] represents the concentration of the protonated [Bi(HDOTA)] and $[Bi(H_5DOTP)]$ intermediates. By taking into account all possible pathways and Eq. (S31), the rate of the dissociation of $[Bi(DOTA)]^-$ and $[Bi(H_4DOTP)]^-$ can be expressed by Eq. (S35).

$$-\frac{d[\mathrm{BiL}]_t}{dt} = k_d[\mathrm{BiL}]_t = {}^{dis}k_0[\mathrm{BiL}] + {}^{dis}k_H[{}^*\mathrm{Bi(H_xL)}] \qquad (S35)$$

where x=1 and 5 for $[Bi(DOTA)]^-$ and $[Bi(H_4DOTP)]^-$, respectively. Considering the total concentration of the $[Bi(DOTA)]^-$ and $[Bi(H_4DOTP)]^-$ complexes ($[BiL]_t=[BiL]+[{}^*Bi(HL)]$) and the protonation constant of BiL (K^H_{BiL}, Eq. (S33)), the k_d pseudo-first-order rate constants presented can be expressed by Eq. (S36).

$$k_d = \frac{{}^{dis}k_0 + {}^{dis}k_1[\mathrm{H}^+]}{1 + K^{H}_{BiL}[\mathrm{H}^+]} \qquad (S36)$$

wherein ${}^{dis}k_0$, ${}^{dis}k_1 = k_H \times K^H_{BiL}$ and K^H_{BiL} are the rate and protonation constants characterizing the spontaneous and H^+ assisted dissociation of the $[Bi(DOTA)]^-$ and $[Bi(H_4DOTP)]^-$ species. The rate and protonation constants characterizing the transchelation reactions of $[Bi(DOTA)]^-$ complex with AAZTA have been calculated by fitting of the corresponding k_d values presented in Figure S20 to the Eq. (S36). The protonation constant (K^H_{BiL}) of $[Bi(H_4DOTP)]^-$

species is relatively small ($K^{H}_{BiL} < 10$) due to the protonation of the coordinated and weakly basic phosphonate O$^-$ donor atom. Therefore, this protonation process could not be detected in the pH-potentiometric studies of [Bi(DOTP)]$^{5-}$ complex. By taking into account the very low protonation constant of [Bi(H$_4$DOTP)]$^-$ species ($K^{H}_{BiL} < 10$), the denominator of Eq. (S36) ($1 >> K^{H}_{BiL}[H^+]$) can be neglected, so Eq. (S36) is simplified in the form of Eq. (S37). The ${}^{dis}k_0$ and ${}^{dis}k_1$ rate constants characterizing the spontaneous and H$^+$ assisted dissociation of the [Bi(H$_4$DOTP)]$^-$ species have been calculated by fitting of the corresponding kinetic data (Figure S20) to Eq. (S37).

$$k_d = {}^{dis}k_0 \quad + \quad {}^{dis}k_1[H^+] \qquad \textit{(S37)}$$

The ${}^{dis}k_0$, ${}^{dis}k_1$ and K^{H}_{BiL} rate and protonation constants characterizing the spontaneous and H$^+$ assisted dissociation of the [Bi(DOTA)]$^-$ and [Bi(H$_4$DOTP)]$^-$ species are shown in Table 3.

IV.3 Transchelation reactions of [Bi(DOTA)]$^-$ and [Bi(DOTP)]$^{5-}$ at high pH (with the use of HP-DO3A^{3-} ligand).

The rates of the transchelation reactions (Eq. (S38)) between Bi^{III} complexes and HP-DO3A^{3-} were studied by CZE at basic condition on the signal of [Bi(HP-DO3A)] (migration time=5.2 min) in the presence of excess of the Bi^{III}-complexes ([Bi(DOTA)]$_{tot}$=[Bi(DOTP)]$_{tot}$=60 mM, [HP-DO3A]$_{tot}$= 5.0 and 10 mM, pH=10.0 – 12.0, 0.15 M NaClO$_4$, 25°C). Some characteristic electropherograms of the [Bi(DOTA)]$^-$ - HP-DO3A^{3-} reacting system are shown in Figure S21.

$$\text{BiL} \ + \ \text{HP-DO3A} \rightleftharpoons \text{Bi(HP-DO3A)} \ + \text{L} \qquad \text{(L=DOTA, DOTP)} \qquad \textit{(S38)}$$

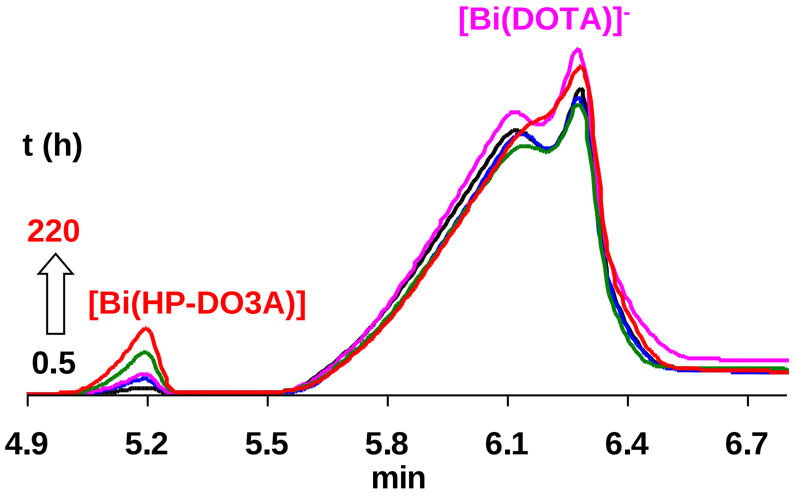

Figure S21. Electropherograms of the [Bi(DOTA)]$^-$ - HP-DO3A^{3-} reacting system at **0.5**, **50**, **60**, **150** and **220** hours after the start of the reaction. ([Bi(DOTA)]$_{tot}$=53.2 mM, [HP-DO3A]$_{tot}$=10 mM, pH=12.0, 10 mM Na$_3$PO$_4$, 0.15 M NaClO$_4$, 25°C).

Under the experimental conditions applied ($[\text{Bi(DOTP)}]_{\text{tot}}$=60 mM, $[\text{HP-DO3A}]_{\text{tot}}$=5 and 10 mM) and at pH between 10.0 – 12.0, the transchelation of $[\text{Bi(DOTP)}]^{5-}$ with HP-DO3A^{3-} does not occur indicating the outstanding inertness of the given complex. In the presence of excess of the Bi$^{\text{III}}$-complexes the transchelation of $[\text{Bi(DOTA)}]^{-}$ can be treated as a pseudo-first-order process and the rate of reactions can be expressed with the Eq. (S28). The rates of the transchelation reactions of $[\text{Bi(DOTA)}]^{-}$ were studied at different concentrations of the HP-DO3A^{3-} ligand in the pH range 10.0 – 12.0. The pseudo-first order rate constants (k_{d}) obtained from the integral values of [Bi(HP-DO3A)] by Eq. (S29) are presented in Figure S22 as a function of pH and $[\text{OH}^-]$.

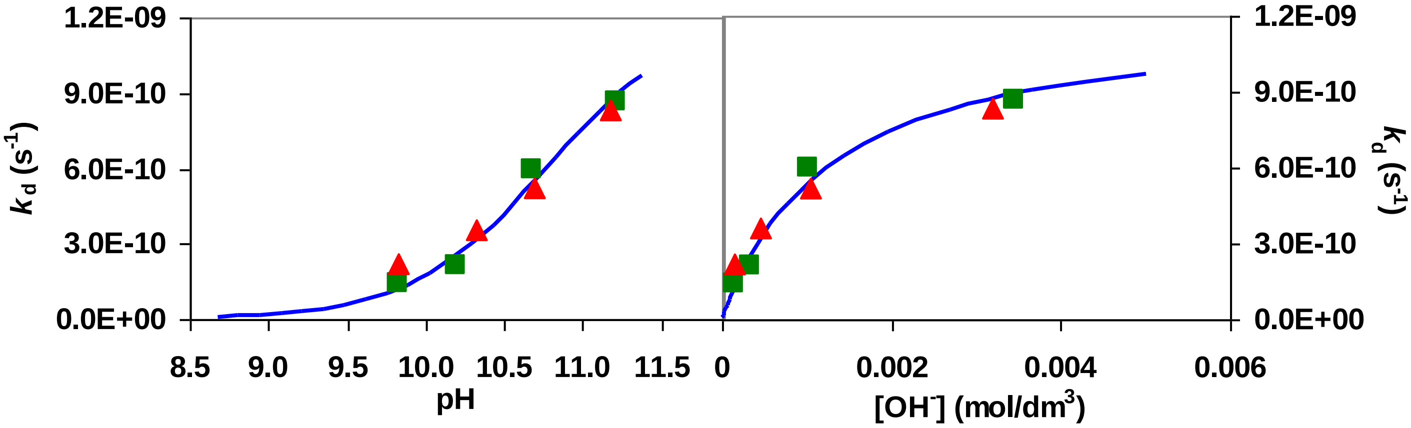

Figure S22. k_{d} pseudo-first-order rate constant characterizing the transchelation reactions of **$[\text{Bi(DOTA)}]^{-}$** with HP-DO3A^{3-} ligand. The solid lines and the symbols represent the calculated and measured k_{d} rate constants. ($[\text{Bi(DOTA)}]^{-}_{\text{tot}}$=60 mM, $[\text{HP-DO3A}]_{\text{tot}}$=5.0 mM (■) and 10 mM (▲) $[\text{Na}_3\text{PO}_4]_{\text{tot}}$=0.01 M, 0.15 M NaClO$_4$, 25°C).

The kinetic data presented in Figure S22 show that the k_{d} values are independent of [HP-DO3A] and increase with pH and $[\text{OH}^-]$, indicating that the rate-determining step of the transchelation reactions is the dissociation of the $[\text{Bi(DOTA)}]^{-}$ complex, followed by the fast reaction between the free Bi$^{\text{III}}$ ion and the exchanging HP-DO3A^{3-} ligand. The dependence of the k_{d} values on pH can be interpreted by the formation ($K^{\text{H}}_{\text{BiLH-1}}$ Eq. (S39)) and the spontaneous dissociation of the $^{*}[\text{Bi(DOTA)H}_{-1}]^{2-}$ intermediate species ($^{\text{dis}}k_{\text{OH}}$, Eq. (S40). The formation of $^{*}[\text{Bi(DOTA)H}_{-1}]^{2-}$ intermediate species might be interpreted by the substitution of the carboxylate O$^-$ donor atom by the OH$^-$ ion in the inner sphere of the Bi$^{\text{III}}$-ion.

$$^{*}\text{BiLH}_{-1} + \text{H}^{+} \overset{K^{\text{H}}_{\text{BiLH-1}}}{\rightleftharpoons} \text{BiL} \qquad (S39)$$

$$K^{H}_{BiLH-1} = \frac{[BiL]}{[*BiLH_{-1}][H^{+}]}$$

$$BiLH_{-1} \xrightarrow{^{dis}k_{OH}} Bi^{3+} + L + OH^{-} \qquad (S40)$$

By taking into account all possible pathways and Eq. (S28), the rate of the dissociation of $[Bi(DOTA)]^{-}$ can be expressed by Eq. (S41).

$$-\frac{d[BiL]_t}{dt} = k_d[BiL]_t = {}^{dis}k_{OH}[*BiLH_{-1}] \qquad (S41)$$

Considering the total concentration of the $[Bi(DOTA)]^{-}$ complex ($[BiL]_t$=[BiL]+$[*BiLH_{-1}]$) and the protonation constant of $*[Bi(DOTA)H_{-1}]^{2-}$ intermediate species (K^{H}_{BiLH-1}, Eq. (S39)), the k_d pseudo-first-order rate constants presented can be expressed by Eq. (S42).

$$k_d = \frac{^{dis}k_{OH}}{1 + K_{BiLH_{-1}}[H^{+}]} \qquad (S42)$$

wherein K^{H}_{BiLH-1} and $^{diss}k_{OH}$ are the equilibrium and rate constants characterizing the formation and the spontaneous dissociation of $*[Bi(DOTA)H_{-1}]^{2-}$ intermediate species. The rate and protonation constants characterizing the transchelation reactions of $[Bi(DOTA)]^{-}$ complex with HP-DO3A have been calculated by fitting the k_d values presented in Figure S22 to the Eq. (S42). The K^{H}_{BiLH-1} and $^{diss}k_{OH}$ protonation and rate constants characterizing the formation and the spontaneous dissociation of $*[Bi(DOTA)H_{-1}]^{2-}$ intermediate species are shown in Table 3.

V. Radiolabeling of DOTA with ^{213}Bi isotope in the presence of citrate, acetate and MES buffers

V.1. Experimental

$^{213}Bi^{III}$ was eluted with a mixture of 0.1 M aq. HCl (0.3 mL) and 0.1 M aq. NaI (0.3 mL) from a ^{225}Ac/^{213}Bi generator system with an initial activity of 15–20 MBq (equivalent to approx. 0.08–0.12 pmol) as provided by the Institute for Transuranium Elements (Karlsruhe, Germany).[26] The eluate was diluted with water (1 mL) and either 3 M ammonium acetate (100 µL) or 1 M sodium 2-(*N*-morpholino)ethanesulfonate (MES, 100 µL) was added, resulting in pH values of 5.2 and 5.6, respectively. The influence of the various anion combinations on the radiolabeling was investigated by determining the fraction of $^{213}Bi^{III}$ complexed by DOTA for different concentrations of DOTA (0.3–100 µM) and citrate (0–100 µM) at 25 °C in 0.14 M ammonium acetate or 0.05 M MES solutions. Labeling was performed by addition of the buffered eluate (80 µL) into an Eppendorf cup containing 10 µL DOTA and 10 µL citrate solutions, resulting in final DOTA and citrate concentrations of 0.3–

100 and 0–100 µM, respectively. After 10 min of incubation at ambient temperature (25 °C), the fraction of complexed $^{213}Bi^{III}$ was evaluated by radio-TLC. For radio-TLC, 0.1 M aqueous trisodium citrate was used as a mobile phase on silica-impregnated glass fibre material (Agilent ITLC®), which deposits any non-complexed ^{213}Bi in form of its citrate complexes near the eluent front ($R_f > 0.8$) while $[Bi(DOTA)]^-$ stays near the origin ($R_f = 0.1$).

VI. Structure of the $[Bi(DOTP)]^{5-}$ complex in solution

VI.1 Experimental

^{1}H, ^{13}C and ^{31}P NMR measurements were performed with the Bruker Avance III (9.4 T) spectrometer, equipped with Bruker Variable Temperature Unit (BVT), Bruker Cooling Unit (BCU) and a BB inverse *z* gradient probe (5 mm). The ^{1}H and ^{31}P NMR chemical shifts of $DOTP^{8-}$ were determined as a function of pH to evaluate some of the protonation constants of the ligand. For these experiments, a 0.01 M solution of H_8DOTP in 0.15 M $NaClO_4$ aqueous solution was prepared (a capillary with D_2O was used for lock). The pH was adjusted by stepwise addition of a solution of NaOH and HCl (both prepared in H_2O). At pH>12, the -log[H^+] values of the samples were adjusted to 0.1, 0.3, 0.6 and 1.0 M with the addition of calculated amounts of 3.0 M NaOH solution (ionic strength was not constant in these samples). ^{1}H and ^{31}P NMR spectra of samples at pH>12 The chemical shifts are reported in ppm, relative to DSS for ^{1}H and ^{13}C and 85% H_3PO_4 for ^{31}P as the external standard. The protonation constants were determined by fitting of the chemical shift versus pH data using *Micromath Scientist, version 2.0* (Salt Lake City, UT) VT- NMR spectra of $[Bi(DOTP)]^{-}$ were measured in 0.1 M samples prepared at pD=10 in D_2O. The ^{1}H-^{1}H correlation spectroscopy (COSY) and exchange spectroscopy (EXSY) spectra were collected by using gradient pulses in the z direction with the standard Bruker pulse program. The ^{1}H - ^{13}C correlation spectra were recorded by using gradient pulse in the z direction with the usual Bruker heteronuclear single quantum coherence (HSQC) pulse sequence. Band-shape analyses were performed by using the *DNMR* program included in the *Bruker Topspin* software package. The ^{31}P NMR signals of H_6DOTP and ^{13}C NMR signals of $[Bi(DOTP)]^{5-}$ were simulated. Values of the chemical shift, the spin-spin coupling constants, intensity and LB values without chemical exchange were fixed input parameters during the fitting procedure. Co-plotting the measured and calculated ^{31}P NMR and ^{13}C NMR spectra obtained at different temperature the similarity was found to be >92%.

VI.2 ^{1}H, ^{13}C and ^{31}P NMR studies of $[Bi(DOTP)]^{5-}$ complex.

In order to acquire deeper insight into the solution structure of $[Bi(DOTP)]^{5-}$, multinuclear 1D and 2D NMR studies have been performed.. 1D and 2D NMR studies of [Bi(DOTP)]- obtained in the temperature range 273 - 333 K are shown in Figures 6, 7, S23 – S28. ^{1}H and ^{13}C NMR signals of the $[Bi(DOTP)]^{5-}$ were assigned on the basis of ^{1}H – ^{1}H COSY (Figure S24), ^{1}H – ^{1}H EXSY (Figure S25) and ^{1}H – ^{13}C HSQC (Figure S26) techniques at 273 and

298K. Structure and the possible conformation of the $[Bi(DOTP)]^{5-}$ with the assignment of the ^{1}H and ^{13}C NMR signals are shown in Scheme 4. The methylene phosphonate protons (3H) of $[Bi(DOTP)]^{5-}$ give two multiplets (ABX, where X is ^{31}P nucleus) with chemical shifts of 2.90 and 3.10 ppm. The ^{31}P nuclei (T_1=1.02 ± 0.05 s at 298 K) are coupled to the two methylene phosphonate protons, with $^{2}J_{HP}$ couplings of – 15.4 and - 15.7 Hz. The ring exhibits four proton signals: $1H_a$ at 2.55 ppm (a doublet with $^{2}J_{HH}\{1H_e\}$=13.6 Hz), $1H_e$ at 3.04 ppm (a "pseudotriplet" with $^{2}J_{HH}\{1H_a\}$=14.5 Hz and $^{3}J_{HH}\{2H_e\}$=14.3 Hz; i.e., the geminal and the vicinal coupling constants are very similar), $2H_a$ at 2.65 ppm (a doublet with $^{2}J_{HH}\{2H_e\}$=13.6 Hz), $2H_e$ at 3.65 ppm (a "pseudotriplet" with $^{2}J_{HH}\{2H_a\}$=13.2 Hz and $^{3}J_{HH}\{1H_e\}$ = 13.3 Hz). The vicinal $^{2}J_{HH}$ and geminal $^{3}J_{HH}$ coupling constants of $[Bi(DOTP)]^{5-}$ are very similar to those of $[Ln(DOTP)]^{5-}$, $[Bi(DOTA)]^{-}$ and $[Ln(DOTA)]^{-}$ complexes.[27–29] The ^{31}P NMR spectra of the $[Bi(DOTP)]^{5-}$ complex is shifted by +1.6 ppm with the respect to the ^{31}P NMR signal of the free $DOTP^{8-}$ ligand as a result of complex formation. $\Delta\delta_P$ value of $[Bi(DOTP)]^{5-}$ is somewhat lower than those of $[Ln(DOTP)]^{5-}$ complexes ($[La(DOTP)]^{5-}$: $\Delta\delta_P$=+7.2 ppm; $[Lu(DOTP)]^{5-}$: $\Delta\delta_P$ =+8.7 ppm).[28] $[Bi(DOTP)]^{5-}$ has a relative simple ^{13}C NMR spectrum with a doublet for the methylene phosphonate 3C carbon (doublet with $^{1}J_{CP}$ = 136.5 Hz), a doublet for the ring 1C carbon (doublet with $^{3}J_{C1P}$ = 16.7 Hz) and a broad singlet for the C2 carbon ($^{3}J_{C2P}$ < 2 Hz). The T_1 relaxation time of the ^{13}C nuclei was found to be 0.12 ± 0.01 s at 298 K. By taking into account the coupling constants of the ring 1C and 2C carbons with ^{31}P nucleus ($^{3}J_{C1P}$ = 16.7 Hz and $^{3}J_{C2P}$ < 2 Hz), the dihedral angles (ϕ) of the 1C – N – 3C – P and 2C – N – 3C – P bonds have been calculated by using the Karplus equation as follows: $^{3}J_{CP} = 17.3\cos^{2}\phi - 4.7\cos\phi - 0.9$.[30] The dihedral angles were found to be ϕ = 46.7° and 151.8° for 2C – N – 3C – P and 1C – N – 3C – P "fragments".

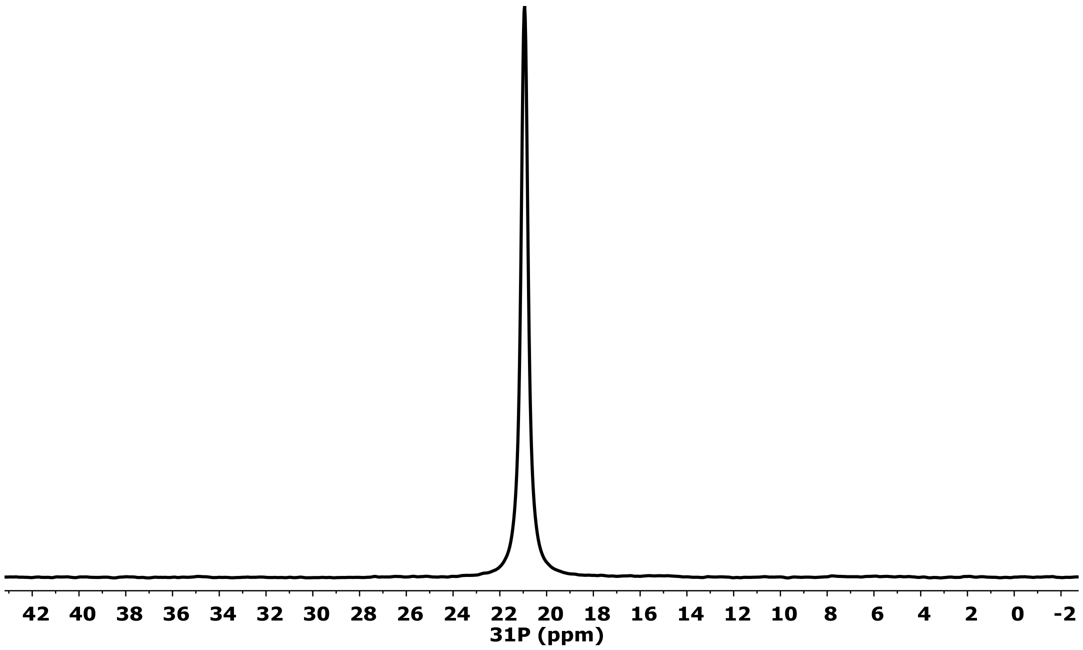

Figure S23. 162 MHz ^{31}P NMR spectra of $[Bi(DOTP)]^{5-}$ at pD=10.0 and 273K ($[BiL]_{tot}$=0.1 M, , D_2O)

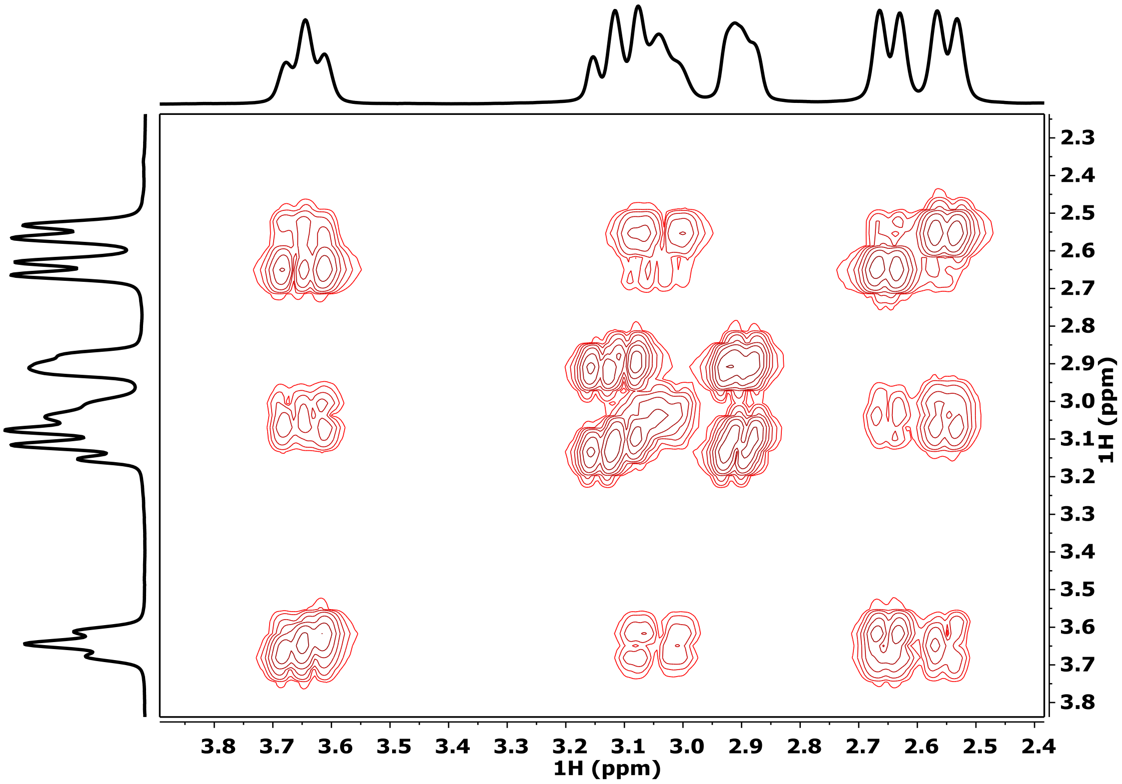

Figure S24. ^{1}H – ^{1}H COSY spectra of $[Bi(DOTP)]^{5-}$ at pD=10.0 and 273K ($[BiL]_{tot}$=0.1 M, D_2O)

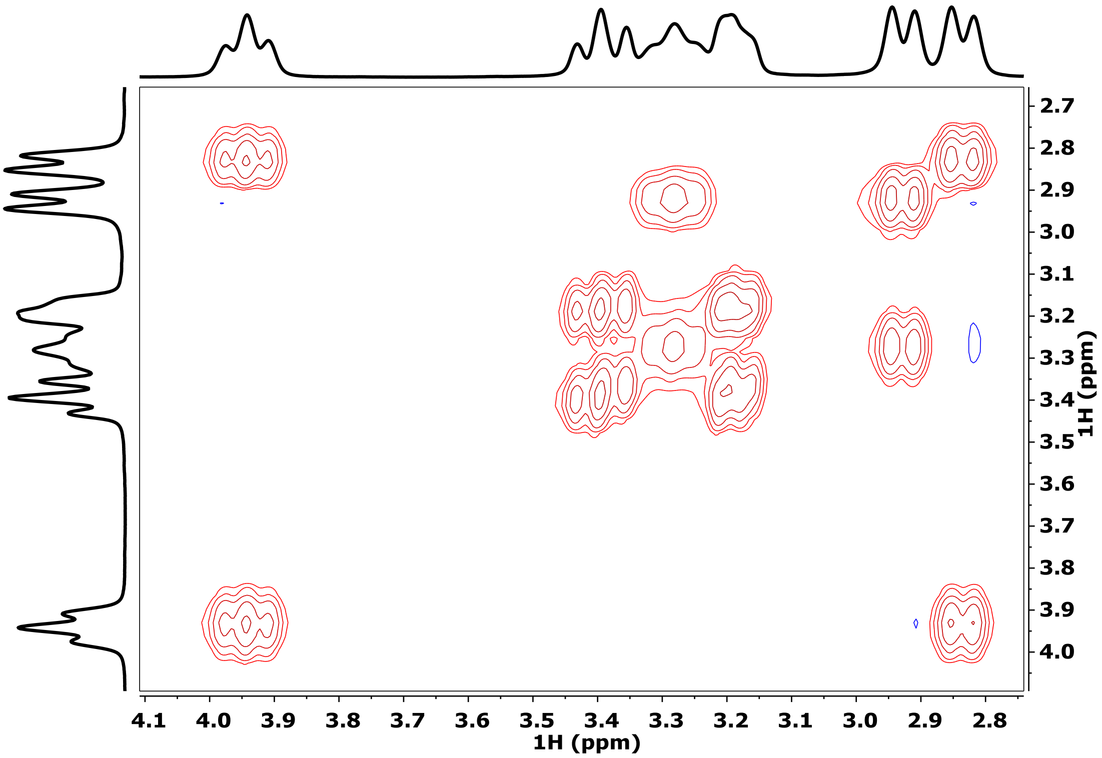

Figure S25. ^{1}H – ^{1}H EXSY spectra of $[Bi(DOTP)]^{5-}$ at pD=10.0 and 298 K ($[BiL]_{tot}$=0.1 M, mixing time D8=50 ms, D_2O)

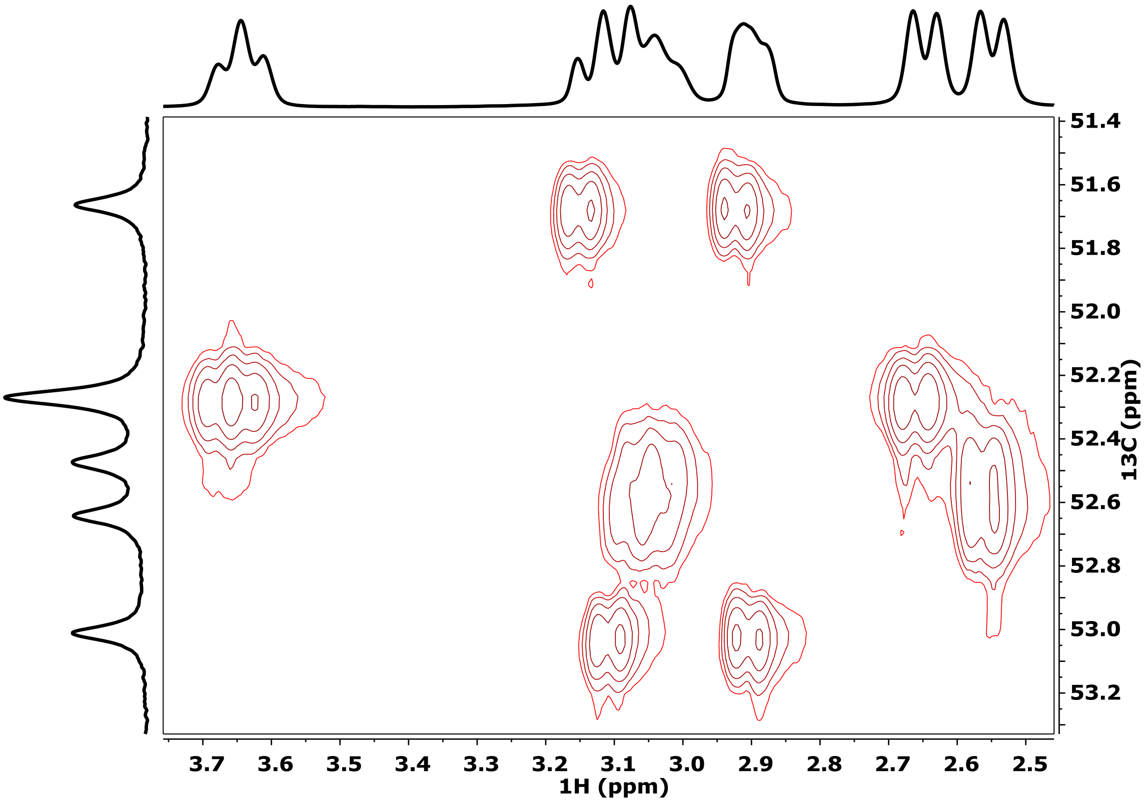

Figure S26. ^{1}H – ^{13}C HSQC of $[Bi(DOTP)]^{5-}$ at pH=10.0 and 273K ($[BiL]_{tot}$=0.1 M, D_2O)

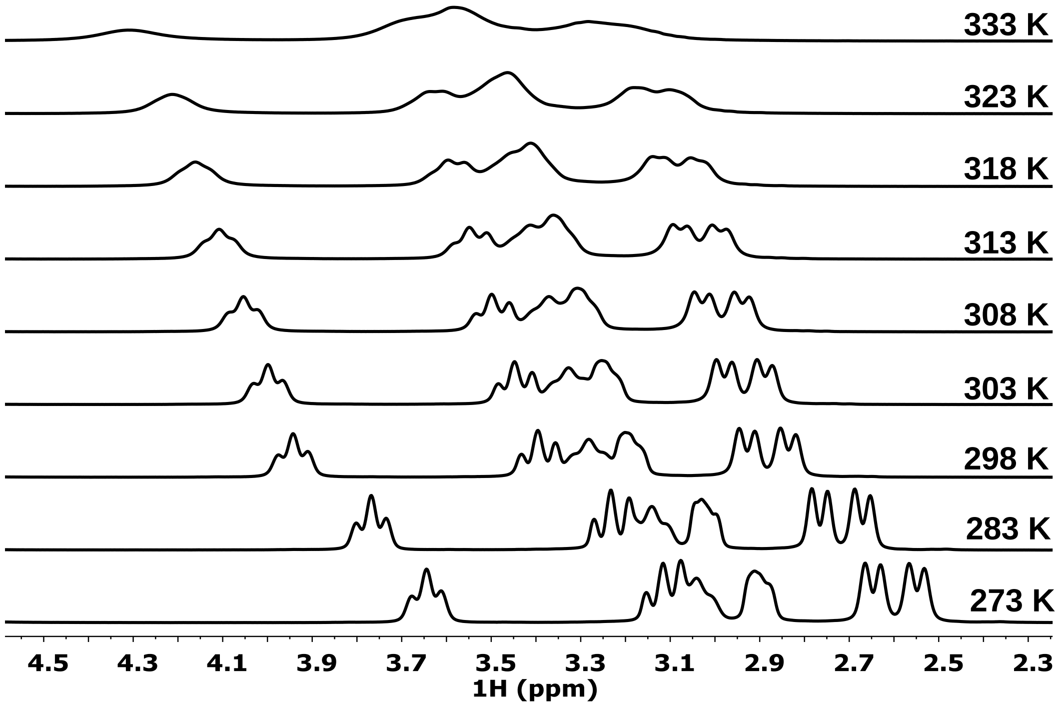

Figure S27. VT-^{1}H NMR spectra $[Bi(DOTP)]^{5-}$ in the temperature range 273-333 K ($[BiL]_{tot}$ = 0.1 M, 400 MHz, pD=10.0, D_2O).

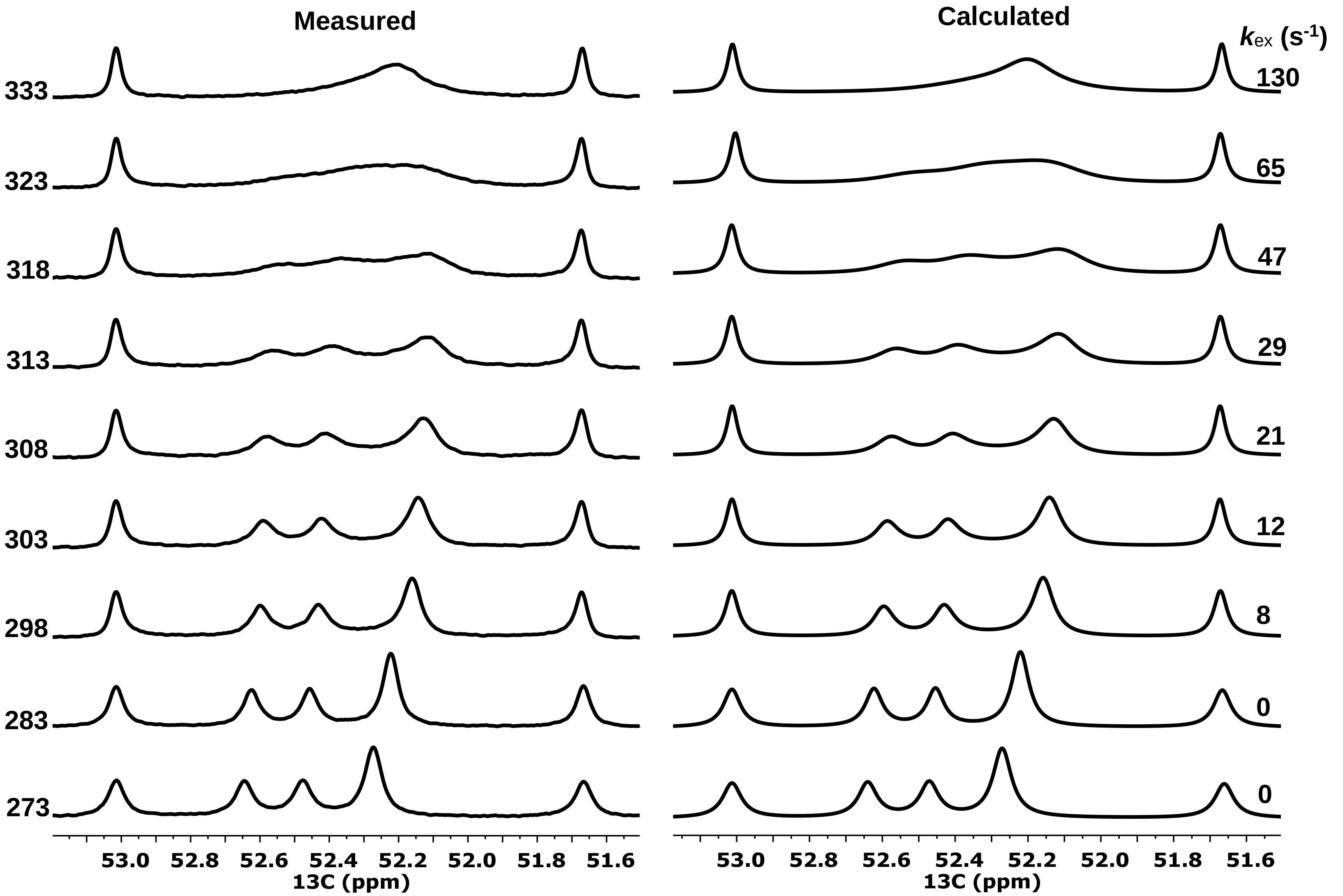

Figure S28. Measured and calculated VT-^{13}C NMR spectra of [Bi(DOTP)]$^{5-}$ in the temperature range 273-333 K ($[BiL]_{tot}$ = 0.1 M, 100 MHz, pD=10.0, D_2O).

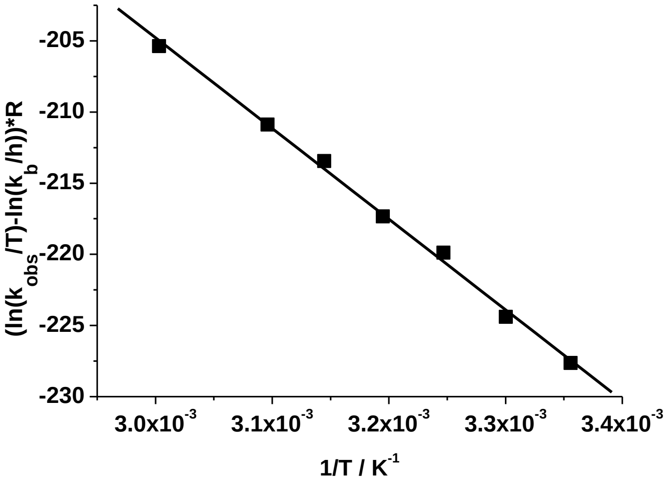

Figure S29. *Eyring* plot for determining the activation parameters of the ring inversion processes of $[Bi(DOTP)]^{5-}$.

VII. References

1 I. Lazar, D. C. Hrncir, W. D. Kim, G. E. Kiefer and A. D. Sherry, Optimized Synthesis, Structure, and Solution Dynamics of 1,4,7,10-Tetraazacyclododecane-1,4,7,10-tetrakis(methylenephosphonic acid) (H_8DOTP), *Inorg. Chem.*, 1992, **31**, 4422–4424, DOI: 10.1021/ic00047a034.

2 S. Aime, L. Calabi, C. Cavallotti, E. Gianolio, G. B. Giovenzana, P. Losi, A. Maiocchi, G. Palmisano and M. Sisti, $[Gd\text{-}AAZTA]^-$: A New Structural Entry for an Improved Generation of MRI Contrast Agents, *Inorg. Chem.*, 2004, **43**, 7588–90, DOI: 10.1021/ic0489692.

3 H. M. Irving, M. G. Miles and L. D. Pettit, A study of some problems in determining the stoicheiometric proton dissociation constants of complexes by potentiometric titrations using a glass electrode, *Anal. Chim. Acta*, 1967, **38**, 475–488, DOI: 10.1016/S0003-2670(01)80616-4.

4 L. Zekany and I. Nagypal, in *Computational Methods for the Determination of Formation Constants*, ed. D. Leggett, Springer US, 1985, pp. 291–353.

5 J. L. Submeier and C. N. Reilley, Nuclear Magnetic Resonance Studies of Protonation of Polyamine and Aminocarboxylate Compounds in Aqueous Solution, *Anal. Chem.*, 1964, **36**, 1698–1706, DOI: 10.1021/ac60215a006.

6 B. P. Karadakov and D. I. Venkova, The complexes of bismuth(III) and nitrilotriacetic acid, *Talanta*, 1970, **17**, 878–883, DOI: 10.1016/0039-9140(70)80184-9.

7 Z. Baranyai, Z. Palinkas, F. Uggeri and E. Brucher, Equilibrium Studies on the Gd^{3+}, Cu^{2+} and Zn^{2+} Complexes of BOPTA, DTPA and DTPA-BMA Ligands: Kinetics of Metal-Exchange Reactions of $[Gd(BOPTA)]^{2-}$, *Eur. J. Inorg. Chem.*, 2010, 1948–1956, DOI: 10.1002/ejic.200901261.

8 S. Chaves, R. Delgado and J. J. Da Silva, The stability of the metal complexes of cyclic tetra-aza tetra-acetic acids, *Talanta*, 1992, **39**, 249–254, DOI: 10.1016/0039-9140(92)80028-c.

9 R. Delgado, J. Costa, K. P. Guerra, L. M. P. Lima, Lanthanide complexes of macrocyclic derivatives useful for medical applications, *Pure Appl. Chem.*, 2005 **77**, 569-579, DOI: 10.1351/pac200577030569.

10 J. F. Desreux, E. Merciny and M. F. Loncin, Nuclear Magnetic-Resonance and Potentiometric Studies of the Protonation Scheme of 2 Tetraaza Tetraacetic Macrocycles, *Inorg. Chem.*, 1981, **20**, 987–991, DOI: 10.1021/ic50218a008.

11 A. Takács, R. Napolitano, M. Purgel, A. C. Benyei, L. Zekany, E. Brucher, I. Tóth, Z. Baranyai and S. Aime, Solution Structures, Stabilities, Kinetics, and Dynamics of DO3A and DO3A–Sulphonamide Complexes, *Inorg. Chem.*, 2014, **53**, 2858–72, DOI: 10.1021/ic4025958.

12 A. Bianchi, L. Calabi, C. Giorgi, P. Losi, P. Mariani, P. Paoli, P. Rossi, B. Valtancoli and M. Virtuani, Thermodynamic and structural properties of Gd^{3+} complexes with functionalized macrocyclic ligands based upon 1,4,7,10-tetraazacyclododecane, *J. Chem. Soc., Dalton Trans.*, 2000, 697–705, DOI: 10.1039/A909098C.

13 R. Delgado and J. J. da Silva, Metal complexes of cyclic tetra-azatetra-acetic acids, *Talanta*, 1982, **29**, 815–22, DOI: 10.1016/0039-9140(82)80251-8.

14 M. T. Beck and I. Nagypal, *Chemistry of Complex Equilibria*, Horwood, 1990.

15 C. F. Baes and R. E. Mesmer, *The Hydrolysis of Cations*, John Wiley & Son, New York, London, Sydney, Toronto, 1976.

16 L. Burai, I. Fábián, R. Király, E. Szilágyi and E. Brücher, Equilibrium and kinetic studies on the formation of the lanthanide(III) complexes, $[Ce(dota)]^-$ and $[Yb(dota)]^-$

(H_4dota = 1,4,7,10-tetraazacyclododecane-1,4,7,10-tetraacetic acid), *J. Chem. Soc., Dalton Trans.*, 1998, 243–248, DOI: 10.1039/A705158A.

17 L. Burai, R. Kiraly, I. Lazar and E. Brucher, Formation and Dissociation Kinetics of the Complexes Gd(DOTP)$^{5-}$ and Gd(DOTPMB)$^{-}$, *Eur. J. Inorg. Chem.*, 2001, 813–820, DOI: 10.1002/1099-0682(200103)2001:3<813::AID-EJIC813>3.0.CO;2-6.

18 M. Perez-Malo, G. Szabo, E. Eppard, A. Vagner, E. Brucher, I. Toth, A. Maiocchi, E. H. Suh, Z. Kovacs, Z. Baranyai and F. Rösch, Improved Efficacy of Synthesizing *M^{III}-Labeled DOTA Complexes in Binary Mixtures of Water and Organic Solvents. A Combined Radio- and Physicochemical Study, *Inorg. Chem.*, 2018, **57**, 6107–6117, DOI: 10.1021/acs.inorgchem.8b00669.

19 P. M. May, D. R. Williams, P. W. Linder and R. G. Torrington, The use of glass electrodes for the determination of formation constants—I A definitive method for calibration, *Talanta*, 1982, **29(4)**, 249–256, DOI: 10.1016/0039-9140(82)80108-2.

20 D. R. Williams, Analytical and computer simulation studies of a colloidal bismuth citrate system used as an ulcer treatment, *J. Inorg. Nucl. Chem.*, 1977, **39**, 711–714, DOI: 10.1016/0022-1902(77)80600-3.

21 J. F. Morfin and E. Toth, Kinetics of Ga(NOTA) Formation from Weak Ga-Citrate Complexes, *Inorg. Chem.*, 2011, **50**, 10371–10378, DOI: 10.1021/ic201445e.

22 Z. Baranyai, Z. Palinkas, F. Uggeri, A. Maiocchi, S. Aime and E. Brucher, Dissociation Kinetics of Open-Chain and Macrocyclic Gadolinium(III)-Aminopolycarboxylate Complexes Related to Magnetic Resonance Imaging: Catalytic Effect of Endogenous Ligands, *Chem. Eur. J.*, 2012, **18**, 16426–16435, DOI: 10.1002/chem.201202930.

23 É. Tóth, R. Király, J. Platzek, B. Radüchel and E. Brücher, Equilibrium and kinetic studies on complexes of 10-[2,3-dihydroxy-(1-hydroxymethyl)-propyl]-1,4,7,10-tetraazacyclododecane-1,4,7-triacetate, *Inorg. Chim. Acta*, 1996, **249**, 191–199, DOI: 10.1016/0020-1693(96)05094-3.

24 E. Toth, E. Brucher, I. Lazar and I. Tóth, Kinetics of Formation and Dissociation of Lanthanide(III)-DOTA Complexes, *Inorg. Chem.*, 1994, **33**, 4070–4076, DOI: 10.1021/ic00096a036.

25 K. Kumar, T. Jin, X. Wang, J. F. Desreux and M. F. Tweedle, Effect of Ligand Basicity on the Formation and Dissociation Equilibria and Kinetics of Gd^{3+} Complexes of Macrocyclic Polyamino Carboxylates *Inorg. Chem.*, 1994, **33**, 3823–3829, DOI: 10.1021/ic00095a028.

26 C. Apostolidis, R. Molinet, G. Rasmussen and A. Morgenstern, *Anal. Chem.*, 2005, **77**, 6288–6291.

27 É. Csajbók, Z. Baranyai, I. Bányai, E. Brücher, R. Király, A. Müller-Fahrnow, J. Platzek, B. Radüchel and M. Schäfer, Production of Ac-225 from Th-229 for targeted alpha therapy, *Inorg. Chem.*, 2003, **42**, 2342–2349, DOI: 10.1021/ac0580114.

28 C. F. G. C. Geraldes, A. D. Sherry and G. E. Kiefer, The solution structure of Ln (DOTP)$^{5-}$ complexes. A comparison of lanthanide-induced paramagnetic shifts with the MMX energy-minimized structure, J. Magn. Reson. (1969), 1992, **97**, 290–304, DOI: 10.1016/0022-2364(92)90314-W.

29 S. Aime, M. Botta and G. Ermondi, NMR study of solution structures and dynamics of lanthanide(III) complexes of DOTA, *Inorg. Chem.*, 1992, **31**, 4291–4299, DOI: 10.1021/ic00047a016.

30 L. D. Quin, M. J. Gallagher, G. T. Cunkle and D. B. Chesnut, Phosphorus-31 and carbon-13 NMR spectra of 2-norbornyl phosphorus compounds. Karplus equations for 3JPC in several phosphorus(III) and phosphorus(IV) derivatives *J. Am. Chem. Soc.*, 1980, **102**, 3136–3143, DOI: 10.1021/ja00529a042.